

DANISH METEOROLOGICAL INSTITUTE

SCIENTIFIC REPORT

03-15

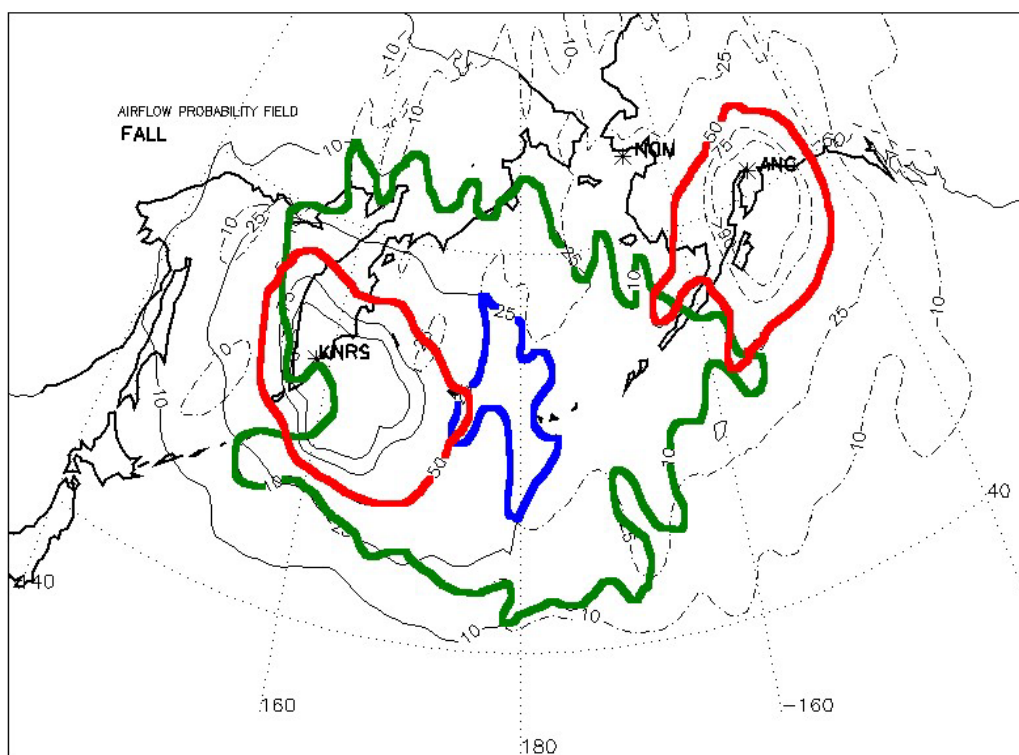
Evaluation of Source-Receptor Relationship for Atmospheric Pollutants Using Trajectory Modelling and Probability Fields Analysis

Alexander Mahura^{1,2} and Alexander Baklanov¹

¹ Danish Meteorological Institute, Copenhagen, Denmark

² Institute of Northern Environmental Problems, Kola Science Centre, Apatity, Russia

Pilot Study



COPENHAGEN 2003

ISSN: 0905-3263 (printed)
ISSN: 1399-1949 (online)
ISBN: 87-7478-489-7

TABLE OF CONTENTS

SUMMARY	2
I. INTRODUCTION	3
II. METHODOLOGY FOR EVALUATION OF SOURCE-RECEPTOR RELATIONSHIP BASED ON TRAJECTORY MODELLING	6
2.1. FORWARD AND BACKWARD TRAJECTORY MODELLING	6
2.2. TRAJECTORY CLUSTER ANALYSIS	11
2.3. PROBABILITY FIELDS ANALYSIS OF TRAJECTORY MODELLING RESULTS	13
III. RESULTS AND DISCUSSION	17
3.1. USING INDIVIDUAL BACKWARD/ FORWARD TRAJECTORIES TO IDENTIFY POTENTIAL SOURCE/ RECEPTOR REGIONS FOR RECEPTOR/ SOURCE POINTS	17
3.2. CLUSTERING OF BACKWARD TRAJECTORIES TO IDENTIFY POTENTIAL SOURCE REGIONS FOR RECEPTOR POINTS	21
3.3. CLUSTERING OF FORWARD TRAJECTORIES TO IDENTIFY POTENTIAL RECEPTOR REGIONS FOR SOURCE POINTS	26
3.4. COMBINED ANALYSIS OF FORWARD-BACKWARD TRAJECTORIES FOR IDENTIFICATION OF SOURCE-RECEPTOR RELATIONSHIP	27
3.5. PROBABILISTIC FIELDS ANALYSIS FOR SOURCE POINTS TO IDENTIFY RECEPTOR REGIONS	29
3.6. PROBABILISTIC FIELDS ANALYSIS FOR RECEPTOR POINTS TO IDENTIFY SOURCE REGIONS	31
3.7. COMBINED ANALYSIS OF PROBABILISTIC FIELDS FOR IDENTIFICATION OF SOURCE- RECEPTOR RELATIONSHIP	33
CONCLUSIONS AND RECOMMENDATIONS	36
ACKNOWLEDGMENTS	39
REFERENCES	40

SUMMARY

In this pilot study we analysed different approaches to evaluate statistically source-receptor relationship for potential atmospheric pollutants in the Euro-Arctic and North Pacific regions. Among source points the risk sites of potential danger were considered, among receptor points the populated cities were selected.

We focused on evaluation of the source-receptor relationship based on trajectory modelling method with a combination of statistical methods (cluster and probability fields) for analyses of modelling results. The approaches for identification and interpretation of potential source and receptor regions were given considering only variability of the atmospheric transport patterns without consideration of possible losses of pollutants during transport. These analyses were presented from different prospective – from a simple point of view to more complex and detailed evaluation of relationship.

First, it is the use of individual backward and forward trajectories originating at selected sites and representing atmospheric transport for a particular date. Second, it is the use of clustered trajectories representing atmospheric transport pathways from and to the sites for a long period. Third, it is the use of airflow probability fields representing spatial and temporal distribution of atmospheric flow patterns from and to the sites. Fourth, it is the use of combined probabilistic fields or sensitivity functions representing both flow patterns and sensitivity of source/ receptor sites with respect to each other.

In order to identify and interpret the source-receptor relationship for atmospheric pollutants we subsequently answered a set of questions: *What occurs **when** a longer period of measurement/ observation records is available and multiple trajectories are considered? What occurs **between** atmospheric transport pathways? What occurs **if** during atmospheric transport the airborne pollutants will undergo the dry and wet deposition processes?* To answer these questions we employed every time another approach which was based on different principles of evaluation and data interpretation. Moreover, the last question is a topic of separate study and report.

The results of this study can be used for the environmental studies, emergency response, decision-making, scientific, educational, and informational purposes by the national and international organisations, programmes, etc. performing monitoring and control of the pollution situation as well as by the administrative, decision-making, etc. services and organizations of local (city, object, site), regional (county, region, territory), governmental (country) levels where sources and receptors of pollution are situated.

I. INTRODUCTION

Estimation of geographical regions and territories with high potential risk/vulnerability from different risk sites is important issue for long-term planning socio-economical development of territories and emergency systems (*INTAS, 2003*). The concept of ecological risk/vulnerability of territories with respect to anthropogenic impact is actively used in recent environmental studies. The problem of risk assessment became especially urgent in connection with different accidents of radioactive, chemical, and biological nature. One of the most important aspects of this problem is the source term estimation for emergency response systems. E.g., after the Algeciras accident in Spain (May of 1998) many European monitoring stations had measured peaks of radiation, but during several days the reason of such peaks was unknown. A similar situation occurred after an accidental release at the Chernobyl nuclear power plant (NPP), Ukraine (April 1996). Such accidents show the importance and necessity to develop constructive methods for estimation of unknown source term based on available monitoring data, prediction and assessment of risk/vulnerability levels for various potential risk sites and situations under conditions of both ordinary and extraordinary anthropogenic loads.

Methods of numerical modelling are widely used for solving of pollution problems including the source-receptor relationship problem. Two main approaches are usually used. The first approach - Lagrangian modelling - allows calculating the trace of individual particle or ensemble of particles moving together with an air mass. The second approach - Eulerian modelling - calculates in a chosen domain the distribution of pollutant concentration released from a set of potential sources. These two approaches are not alternative. They supplement each other, although each approach has its own advantages and shortcomings as well as application areas.

Dependence on a goal of investigation, the forward and inverse procedures of modelling are distinguished. The methods of forward modelling are traditionally used for the solution of forecast problems. For their realization, the values of all model input parameters, boundary and initial conditions, sources of external and internal forcing, etc. should be given. Forward problems are used to study the processes of propagation of perturbations from various sources. These are so-called source-receptor problems. The spatial-time domains, where perturbations are observed, play role of zones-receptors. The methodology of inverse modelling is mainly oriented towards diagnosis and solution of inverse problems. Its value is that it starts from the result (receptor) and moves to the sources and causes. From a viewpoint of ecological safety, inverse problems of the receptor-source type are of interest, since they allowing determine a degree of potential danger of contamination of zone-receptor by pollutants entering it and to identify sources of this danger. In combination with forward modelling, the inverse approach opens a new prospect to extend the class of relevant problems, develop and organize interactive technologies for their control and mitigation.

Source-receptor data can be evaluated: a) statistically or b) in combination with monitoring data to derive sources or other model variables. The common back-trajectory technique, suitable only for Lagrangian models, is an example of such inverse studies. The methodology of source-receptor relations is actively developing. The Novosibirsk Russian scientific school of Prof. G.I. Marchuk had suggested a theoretical method for inverse modelling, based on adjoint equations (*Marchuk, 1982; Marchuk, 1995; Baklanov, 2000*) and suitable for the Eulerian models (*Pudykiewicz, 1998*). Recently (*Penenko et al., 2002; Baklanov, 2000; Penenko & Baklanov, 2001*) suggested theoretical methods for source-term estimation based on variational principles with adjoint equations and suitable for both the Eulerian and Lagrangian models. It is combined with decomposition, splitting, and optimisation techniques for construction of numerical algorithms. The novel aspects are the sensitivity theory and inverse modelling for environmental problems, which use the solution of the corresponding adjoint problems for a given set of models and functionals

(which are criteria of the atmospheric quality and/or informative quality of measurements) (Penenko, 2001a; Penenko, 2001b; Penenko & Tsvetova, 2000).

Rather than doing a full source-receptor calculation, the Chemical transport model data assimilation systems calculates a cost-function - source relationship (in the case that source determination is the task), i.e. the gradient of the cost function with respect to the control variables (Stohl *et al.*, 2002). It works for both the linear and nonlinear problems. For linear source-receptor relationships (and linear cost functions), the optimisation problem of inverse modelling is solved alternatively on the basis of the source-receptor matrix with analytical techniques where matrix can be calculated with the Eulerian as well as Lagrangian particle dispersion models in forward/backward mode (Seibert, 1999; Seibert, 2001). The neural networks approach combined with a set of historical calculations of dispersion models and monitoring network data can also be used for identification of the sources of potential danger (Gorodnichi & Reznik, 1997; Kovalets & Maderich, 2001a; Kovalets & Maderich, 2001b).

The long-term dispersion modelling approach (AR-NARP, 2001-2003; Baklanov *et al.*, 2002) for evaluation of the source-receptor relationship for various pollutants including nuclear, chemical, biological, etc. danger can be realized employing the Danish Emergency Response Model for Atmosphere (DERMA) for different resolutions and grid domains (Sørensen, 1998; Baklanov & Sørensen, 2001). Similarly, the EURAD model system (EUROpean Atmospheric Dispersion model system) employing a four-dimensional variational (4D-var) chemical data assimilation, and advanced scheme for dynamical and chemical aerosol simulation, can be used for evaluation of source-receptor relationship (Hass *et al.*, 1990; Elbern & Schmidt, 1999; Elbern & Schmidt, 2002).

The following aspects, approaches, and methods for investigation of the source-receptor receptor (SRR) problem are of the major interest (INTAS, 2003):

- the source-receptor data can be evaluated statistically for long-term periods or specific cases (i.e. episodes of elevated and lowest concentration of pollutants) in combination with available monitoring data. It will allow to derive potential sources and estimate model parameters;
- the SRR can be studied also employing dispersion approach to simulate forward/ backward individual or multiyear atmospheric transport, dispersion, and deposition datasets for pollutants considered on different scales ranging from local to global;
- the SRR can be investigated employing trajectory approach to calculate forward/ backward individual or multiyear trajectory datasets for the source and receptor sites/regions;
- the SRR can be solved using the adjoint problem methodology based on variational principles, combination of direct and inverse modelling, and sensitivity theory;
- the SRR can be studied employing the cluster analysis techniques over the multiyear trajectory datasets on different temporal (month, season, year) and spatial scales (altitudes of transport, geographical regions);
- the SRR can be analyzed using probability fields analysis of calculated trajectory/ dispersion datasets on temporal and spatial scales;
- moreover, these SRR can be evaluated using GIS methods for assessment of integrated risk and vulnerability of potential source and receptor regions.

We consider in our source-receptor relationship studies different methods for the mentioned above, including adjoint equations for atmospheric dispersion models (e.g. Baklanov, 2000; Penenko & Baklanov, 2001). However, in this study we will focus and concentrate on the trajectory modelling approach which is simpler and less computationally expensive compared with the dispersion modelling approach. At the beginning let us underline where, in general, atmospheric trajectories both forward and backward have found their applicability for different tasks of environmental studies including evaluation of source-receptor relationship. Among the main directions of atmospheric trajectories (*with examples of referred studies*) usage are the following:

- the trajectories can be used to evaluate a general climatology or peculiarities of atmospheric flows within different meteorological systems and over different geographical regions and territories of interest (*Merrill et al., 1985; Harris & Kahl, 1990; Harris, 1992; Katsoulis & Whelpdale, 1993; Merrill, 1994; Harris & Kahl, 1994; Kahl et al., 1997; Jaffe et al., 1997a; Mahura et al., 1997a; Mahura et al., 1998; Mahura & Baklanov, 2003b*).
- the trajectories can be employed to determine directions of atmospheric transport of tracers in various experiments related to studies of atmospheric transport patterns (*Clarke, 1983; Haagenson et al., 1987; Anfossi, 1988; Martin et al., 1990; Sparling et al., 1997*).
- the trajectories can be applied to evaluate relationship between sources and receptors for atmospheric pollutants on different scales: ranging from meso- to global scales (*Slanina & Willem, 1983; Harris et al., 1992; Dorling et al., 1992; Moody et al., 1995; Thompson et al., 1996; Jaffe et al., 1997b; Harris & Oltmans, 1997; Jaffe et al., 1998; Mahura et al., 2003b*).
- the trajectories can be selected for investigation of processes of diffusion, transport, and chemical interactions of pollutants such as, for example, ozone - within the boundary layer, free troposphere, and low stratosphere (*Fosberg, 1984; Bowman, 1995; Chipperfield et al., 1997*).
- the trajectories can be proposed to study exchange by momentum, heat, and humidity, as well as potential pollutants between the troposphere and stratosphere (*Austin & Butchart, 1989; Eluszkiewicz, 1996; Kowol-Santen, 1998*).
- the trajectories can be studied to analyse transboundary and long-range transport of atmospheric pollutants due to removal by precipitation (*Haagenson, 1985; De Pena, 1986; Artz & Dayan, 1986; Moody, 1986; Moody & Galloway, 1988; Ruijgrok & Romer, 1993*).
- the trajectories can be calculated to evaluate specific cases or episodes with the elevated concentrations of pollutants (*Martin et al., 1987; Jaffe et al., 1997b*), including radionuclides (*Puhakka, 1988; Baklanov et al., 2003*), dangerous and representing potential risk the natural (*Schoeberl et al., 1993; Anfossi & Sacchetti, 1994*) and weather (*Janish & Lyons, 1992; Perrin & Simmonds, 1995*) events.
- the trajectories can be modelled to learn the formation and development of different synoptical processes and phenomena (*Uccellini, 1988; Rotunno et al., 1994; Bowman, 1995; Market & Moore, 1998*) including the characteristics of formation of polar stratospheric clouds (*Rizi et al., 1999*).

In this pilot study we will focus on the evaluation of source-receptor relationship based on trajectory modelling approach with a combination of statistical methods (cluster and probability fields) for analyses of modelling results. The aspects of the dispersion and deposition modelling approach (*AR-NARP, 2001-2003; Baklanov et al., 2002*) as well as GIS methods (*AR-NARP, 2001-2003; INTAS, 2003*) for the evaluation of the source-receptor relationship, which are the topics of a separate report, are not considered. Moreover, these are also a part of the submitted proposal INTAS Call-2003: “Source-Receptor Relationships for Atmospheric Pollutants Related to Environmental Risks in the NIS countries – Methodology and Applications” (*INTAS-2003*). The main aim of this proposal is the development of new elements and improvement of methodology for calculation and evaluation of SRR for atmospheric pollution, and application of those for the source term estimation, assessment and prediction of the environmental/health risk and vulnerability for industrialized/populated regions and natural complexes as well as validation via dedicated case studies for selected sites and regions in the European countries.

II. METHODOLOGY FOR EVALUATION OF SOURCE-RECEPTOR RELATIONSHIP BASED ON TRAJECTORY MODELLING

In this section of report the methodological aspects for evaluation of the source-receptor relationship based on employing of the forward/ backward trajectory modelling approach (§2.1) and statistical analyses of trajectory modelling results (§2.2 and 2.3) are discussed.

2.1. FORWARD AND BACKWARD TRAJECTORY MODELLING

Trajectories and Modelling

In general, each computed atmospheric trajectory represents a pathway of an air parcel motion in time and space. There are a few approaches to model atmospheric trajectories. Two of these approaches are commonly used: isobaric and isentropic. The modelling of more realistic trajectories – “fully 3-D trajectories” - is preferable, although it is complex and it requires incorporation into simulation of large number of variables and parameters, and moreover, for the long-term statistics it increases significantly a computational time. In this study the isentropic approach was selected. Although this type of trajectory modelling uses assumption of adiabatically moving air parcels and neglects various physical effects, it is still a useful research tool for evaluating common airflow patterns within meteorological systems on various scales. Some uncertainties in these models are related to the interpolation of meteorological data, which might be sparsely measured, applicability of the considered horizontal and vertical scales, assumptions of vertical transport, etc. (*Merrill et al., 1986; Kahl & Samson, 1986; Kahl & Samson, 1988; Kahl, 1996; Stohl, 1998*).

In this study, the modelling of trajectories was performed in two steps. At the first step, an interpolation procedure was performed for a multiyear period applying a technique described by *Merrill et al., 1986*. The wind components were recalculated from the isobaric system of coordinates - (x, y, p) into the isentropic system of coordinates - (x, y, Θ) through the Decart system of coordinates - (x, y, z) . The angles of slopes of isentropic surfaces are calculated. Let's define the

horizontal derivatives of variables – $\{ \}$ - through $\left(\frac{\partial z}{\partial x} \right)_{\Theta}$ and $\left(\frac{\partial z}{\partial y} \right)_{\Theta}$ in the following way:

$$\left(\frac{\partial \{ \}}{\partial x_z} \right)_{\Theta} = \frac{\partial \{ \}}{\partial x_{\Theta}} - \frac{\partial z}{\partial x_{\Theta}} \frac{\partial \{ \}}{\partial z_x}, \quad \left(\frac{\partial \{ \}}{\partial y_z} \right)_{\Theta} = \frac{\partial \{ \}}{\partial y_{\Theta}} - \frac{\partial z}{\partial y_{\Theta}} \frac{\partial \{ \}}{\partial z_y}.$$

Hence, in equations of horizontal motion for the pressure gradient obtain the following:

$$\frac{1}{\rho} \frac{\partial p}{\partial x_z} = (C_p T_v)_{\Theta} \frac{\partial \{ \}}{\partial x} + (gz)_{\Theta} \frac{\partial \{ \}}{\partial x} = \left(\frac{\partial \Psi_M}{\partial x} \right)_{\Theta},$$

$$\frac{1}{\rho} \frac{\partial p}{\partial y_z} = (C_p T_v)_{\Theta} \frac{\partial \{ \}}{\partial y} + (gz)_{\Theta} \frac{\partial \{ \}}{\partial y} = \left(\frac{\partial \Psi_M}{\partial y} \right)_{\Theta},$$

where:

x, y, z – directions in the Decart system of coordinates,

t – time,

g – gravitational acceleration,

p – pressure,

ρ – air density,

C_p – specific heat capacity of air at constant pressure,

T_v – virtual temperature,

Ψ_M – Montgomery function or potential of Montgomery,

$$\Psi_M = \pi \cdot \Theta + \Phi = \Theta \cdot \left(C_p \left(\frac{p}{p_0} \right)^{\frac{R_c}{C_p}} \right) + \Phi,$$

where:

π – Exner function for pressure,

p_0 – pressure at the reference level of 1000 hPa,

R_c – specific gas constant for the dry air,

Φ – geopotential at the surface Θ .

After definition of the pressure as a function of the potential temperature, the components of wind velocity on the isentropic surfaces will be calculated by linear interpolation on pressure.

At the second step, the components of wind velocity at the isentropic surfaces are used to calculate trajectories of air parcels motion from the sites. The kinematic is used which takes into account only the velocity fields. To calculate the spatial position of air parcel the following numerical evaluation of equations is used:

$$x^{n+1} = x^n + \int_{t^n}^{t^{n+1}} u(x, y, \Theta, t) dt,$$

$$y^{n+1} = y^n + \int_{t^n}^{t^{n+1}} v(x, y, \Theta, t) dt.$$

where:

$x^n, y^n, x^{n+1}, y^{n+1}$ – coordinates of air parcel at moment of time n and $n+1$,

$u(x, y, \Theta, t), v(x, y, \Theta, t)$ – horizontal components of wind velocities on the isentropic surfaces Θ at the time moment t ;

x, y, z – direction of the Decart system of coordinates.

For a particular level of potential temperature, the equation to estimate the path of trajectory is the following:

$$x^{n+1} = x^n + \left[\frac{u(x^n, y^n, t^n) + u(x^{n+1}, y^{n+1}, t^{n+1})}{2} \right] \Delta t,$$

$$y^{n+1} = y^n + \left[\frac{v(x^n, y^n, t^n) + v(x^{n+1}, y^{n+1}, t^{n+1})}{2} \right] \Delta t.$$

Instead of calculating only one trajectory, four trajectories for every calculation were used. The initial points of trajectories are located at each corner of a $1^\circ \times 1^\circ$ of latitude vs. longitude box, where the site is in the centre of the box. Calculation of four trajectories simultaneously allowed evaluating a consistency of the wind field in the direction of the atmospheric transport.

Depending on the purpose of the study the duration of calculated trajectories could be limited. For example, for further statistical analysis the selection of limitation (in days, in hours) will depend on 1) quality and accuracy of trajectory calculations which after 5 days drops significantly, 2) observing development frames of the synoptic scales systems in the regions studied, 3) relative proximity of the analyzed geographical regions from the sites/regions of interest. Moreover, to

study altitudinal variations in the flow patterns (in particular, within the boundary layer and free troposphere), trajectories originated over the site regions at altitudes of 1.5 and 3 km above sea level (asl) could be also considered.

Input Meteorological Datasets

In general, for any trajectory calculation (for a specific date, for a particular period of time, or for a multiyear period) the meteorological data are essential. The useful approach is to use the gridded datasets, i.e. the main atmospheric variables and parameters are calculated in the grids of the latitude vs. longitude domain. In this study, we used two datasets – NCAR (National Center for Atmospheric Research, Boulder, Colorado) and ECMWF (European Center for Medium-range Weather Forecast, Reading, UK) - although we could note that any reliable dataset might be used for trajectory modelling. Moreover, in this study the NCAR dataset was used more often compared with the ECMWF dataset.

The used in this study dataset - DS082.0 - NCEP Global Tropospheric Analyses (from Jul 1976 - present) is one of the major gridded analyses available. It is a part of the operational and gridded analyses performed at the National Center for Environmental Prediction (NCEP; prior to 1995 known as the National Meteorological Center – NMC). This dataset has a resolution of $2.5^\circ \times 2.5^\circ$ latitude vs. longitude (145 x 37 grids) for both Northern and Southern hemispheres. It consists of the surface, tropospheric, tropopause, and lower stratospheric analyses as well as at the standard levels up to 50 millibars (mb). The main analyzed variables are the following: geopotential height, temperature, u-, v-, and w-components of the wind, relative humidity, sea level pressure, surface pressure and temperature, sea surface temperature, snowfall, precipitable water, potential temperature, vertical motion, tropopause pressure and temperature. An analysis has been done on a daily basis at 00 and 12 UTC terms (Universal Coordinated Time).

The meteorological data from the European Centre for Medium-Range Weather Forecasts (ECMWF), Reading, UK are based on the ECMWF's global model forecasts and analyses having a resolution up to $0.5^\circ \times 0.5^\circ$ latitude vs. longitude and 3 hours time interval for both the Northern and Southern hemispheres. It consists of the geopotential, temperature, vertical velocity, u and v components of horizontal wind, relative humidity and specific humidity at each level, etc. Analysis has been done on a daily basis at 00, 06, 12, and 18 UTC terms.

Forward and Backward Trajectories Showing Convergence of Airflow

Although all calculated trajectories can be used for further analysis, it should be noted that there are differences in the representation of the general flow along trajectories. The flow is considered to be a reasonably consistent along the transport path if all four trajectories had shown a similar direction (reflecting convergence of flow) of transport for one time period.

For the cases shown in Fig. 2.1.1, we see that the forward trajectories originated over the regions of the source points (in particular, over the locations of the nuclear risk sites (NRSs) – nuclear power plants (NPPs). During the entire period of atmospheric transport, all trajectories showed a consistent airflow along the direction of transport. For example, as shown in Fig. 2.1.1b, the trajectories originated over the Loviisa NPP region (Finland) at 00 UTC, 19 Jan 1993 within the boundary layer. Initially, during the first three days they moved in the south-eastern direction toward the Caspian Sea, and then in the north-eastern direction toward the Taymyr Peninsula of Russia. The airflow remained stably directed during all days of atmospheric transport. Therefore, such trajectories clearly showed that an air mass originated over the source points was transported to the exact remote region.

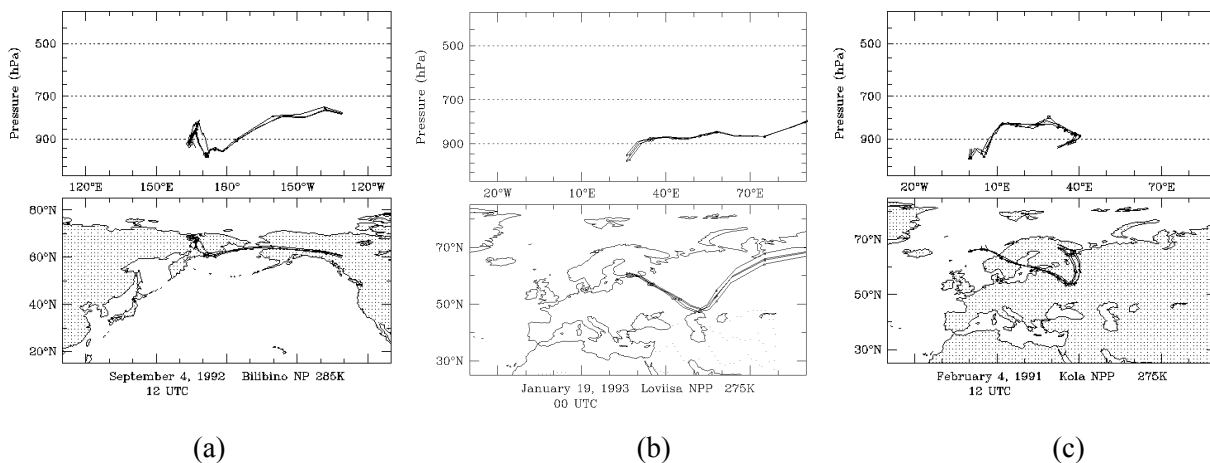


Figure 2.1.1. Isentropic forward trajectories originated at source points and showed a consistent airflow: a) Bilibino NPP, Russia, b) Loviisa NPP, Finland, and c) Kola NPP, Russia.

For the cases shown in Fig. 2.1.2, we see that the backward trajectories arrived to the regions of the receptor points. During the entire period of atmospheric transport, all trajectories showed a relatively consistent airflow along the direction of transport prior to arriving at sites. For example, as shown in Fig. 2.1.2b, the air parcels arrived at Shemya (Aleutian Chain Islands, USA) at 00 UTC, 23 Feb 1994. Initially, the trajectories originated within the free troposphere over the Canadian Arctic territories. During several days they descended in the south-western direction passing over Alaska, which seem to be attributed to the anticyclonic activity. During the last day before arrival at the site, they were over the Bering Sea aquatoria and travelled within the boundary layer. The airflow remained a relatively stable directed during atmospheric transport. Therefore, such trajectories clearly showed that an air mass arrived at the receptor point was transported from the exact remote region.

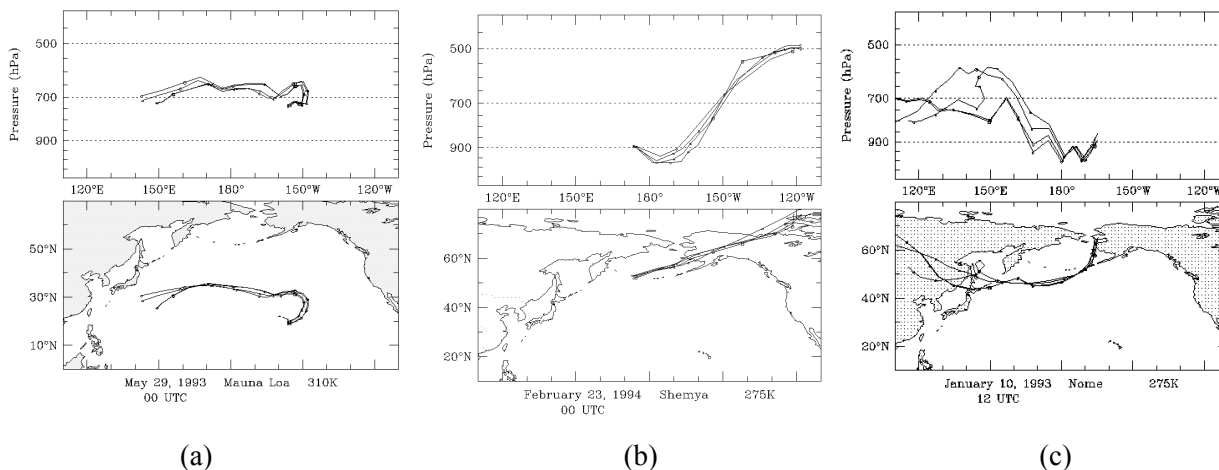


Figure 2.1.2. Isentropic backward trajectories arrived at receptor points and showed a consistent airflow: a) Mauna Loa Observatory, Hawaii, b) Shemya, Alaska, and b) Nome, Alaska.

Forward and Backward Trajectories Showing Divergence of Airflow

Trajectories, showing a strong divergence of flow, are assigned to a category of the “complex trajectories”. These trajectories reflect more uncertainties in the air parcels motion. These

differences are not so important in evaluation of the general climatological patterns, but they can be significant, for example, for identification of source regions for air pollutants, evaluation of the nature of the specific events with recorded elevated concentration of species, tracking tracers in the atmosphere, etc.

For the cases shown in Fig. 2.1.3, we could see that the forward trajectories originated over the regions of the source points showed an inconsistent airflow along the initial direction of atmospheric transport. For example, as shown in Figs. 2.1.3ac, the air parcels originated over the NPPs regions after the first day of transport showed a strong divergence of airflow – clearly seen the transport in opposite directions. In Fig. 2.1.3b, the horizontal divergence of airflow had started after the first day of transport, and it reached further more than 270 degrees. As we see, the airflow does not remain stably directed during the entire period of atmospheric transport. Therefore, such trajectories clearly show that air mass originated over the source points cannot be transported to the exact remote region.

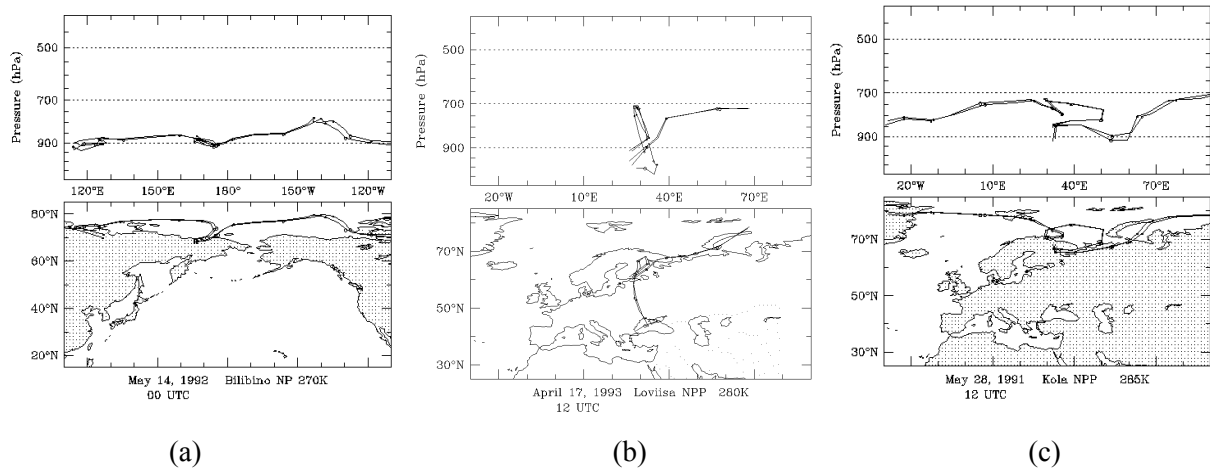


Figure 2.1.3. Isentropic forward trajectories originated at source points and showed a strong divergence of airflow: a) Bilibino NPP, Russia, b) Loviisa NPP, Finland, and c) Kola NPP, Russia.

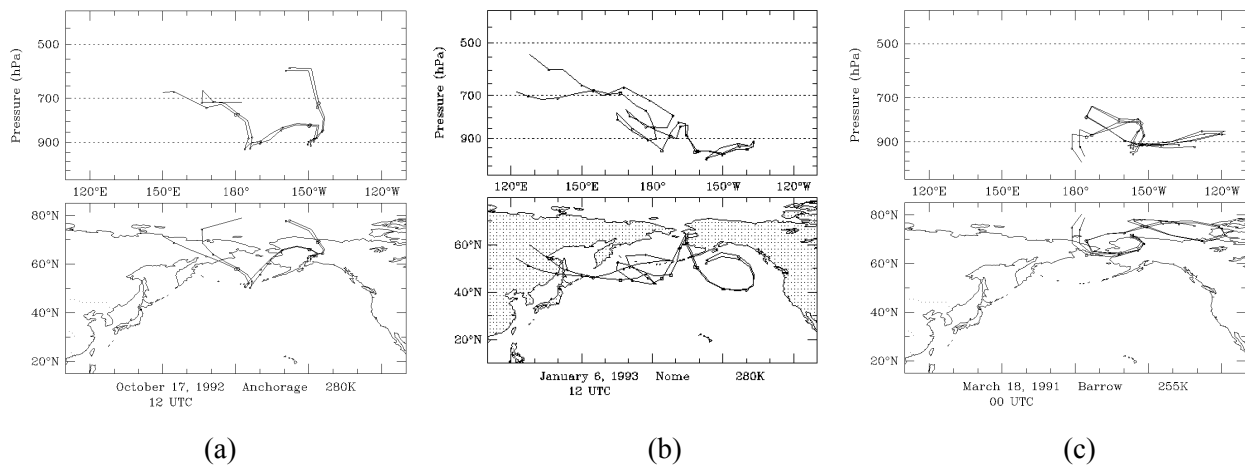


Figure 2.1.4. Isentropic backward trajectories arrived at receptor points and showed a strong divergence of airflow: a) Anchorage, Alaska, b) Nome, Alaska and c) Barrow, Alaska.

We should note that such types of trajectories still could be used for identification of the general atmospheric transport patterns from the source points (or to receptor points) for a multiyear period. This deviation might be removed due to “smoothing” in the large datasets of trajectories. Although, for identification of the source/receptor regions for the specific dates (or cases) it is not appropriate to use such trajectories (in general, a few percent of calculated trajectories). And moreover, it raises a concern about correct assigning, for example, of elevated concentration of chemical species at receptor points.

2.2. TRAJECTORY CLUSTER ANALYSIS

The cluster analysis is a variety of multivariate statistical analysis techniques, which could be used to explore the existing structure within data sets (*Romesburg, 1984*). The specific purpose of this analysis is to divide a data set into groups (or clusters) of similar variables (or cases). *Miller, 1981* initiated application of the cluster analysis on trajectories. The important output of his study was evaluation of the airflow climatology, in particular, over the long time periods. Then later, cluster analysis techniques on trajectories were used extensively by various researchers in different scientific fields.

In general, output of cluster analysis on trajectories can provide insights in the tracers transport, common atmospheric flow patterns for the sites of interest, identification of the source regions for atmospheric pollutants, etc. The cluster analysis is used to divide calculated trajectories into groups, which represent the major airflow transport regimes. The following criteria are used: latitude and longitude values at each time interval of trajectory. These represent both direction and velocity of air parcel motion.

Let us introduce variables X and Y , representing latitude and longitude of trajectory at each time interval, respectively. Then, for example, if 5-day trajectories are considered than there are 11 pairs of values for latitude and longitude, if 10-day trajectories are considered than there are 21 pairs of values for latitude and longitude, etc. To calculate the Euclidean distances $DE(X, Y)$ the following equation is used:

$$DE(X, Y) = \sqrt{\sum_{t=1}^{NT} kw_t (X_t - Y_t)^2},$$

where:

X_t, Y_t - longitude and latitude of trajectories at moment t ($t = 0, NT$ days; $\Delta t = 12$ hours),

NT – number of considered time intervals for trajectories (or number of pairs of values of latitude and longitude),

kw_t - weight coefficient (selected in order to regulate the number of clusters, in the first approximation $kw_t = 1$).

The Euclidean distances will characterize the differences between X and Y . Hence, let us define for these distances the following characteristics – size $DE_{size}(X, Y)$ and shape $DE_{shape}(X, Y)$:

$$DE_{size}(X, Y) = \frac{\left| \sum_{t=1}^{NT} kw_t (X_t - Y_t) \right|}{\sqrt{\sum_{t=1}^{NT} kw_t}},$$

$$DE_{shape}(X, Y) = \sqrt{\sum_{i=1}^{NT} kw_i [(X_i - \bar{X}) - (Y_i - \bar{Y})]^2},$$

$$\bar{X} = \frac{1}{NT} \sum_{t=1}^{NT} X_t, \quad \bar{Y} = \frac{1}{NT} \sum_{t=1}^{NT} Y_t,$$

where:

\bar{X}, \bar{Y} – averaged values of longitude and latitude for trajectories.

The low values of $DE(X, Y)$ and its characteristics show that X and Y are more similar; and the high values show that X and Y are less similar.

At the next step, in order to evaluate similarities between X and Y the following characteristics are calculated:

covariance $COV(X, Y)$:

$$COV(X, Y) = \sum_{t=1}^{NT} kw_t \frac{(X_t - \bar{X}) - (Y_t - \bar{Y})}{DF}, \quad \text{where:} \quad DF = \begin{cases} NT - 1 & \text{if } kw_t = 1 \\ \sum_{t=1}^{NT} kw_t - 1 & \text{if } kw_t \neq 1 \end{cases},$$

and correlation $COR(X, Y)$:

$$COR(X, Y) = \frac{\sum_{t=1}^{NT} kw_t (X_t - \bar{X}) - (Y_t - \bar{Y})}{\sqrt{\sum_{t=1}^{NT} kw_t (X_t - \bar{X})^2 \sum_{t=1}^{NT} kw_t (Y_t - \bar{Y})^2}}.$$

The correlation coefficient $COR(X, Y)$, varying in the interval from +1 to -1, shows the highest similarities between variables if it has the highest positive values. It is used for the evaluation of the order of inter-relationship between X and Y .

The covariance $COV(X, Y)$ shows the joint variability (or variance) of both variables X and Y with respect to the joint average. The higher values of covariance show the higher order of relationship between variables. If additional variables are included than correlation and covariance are calculated for all pairs of variables.

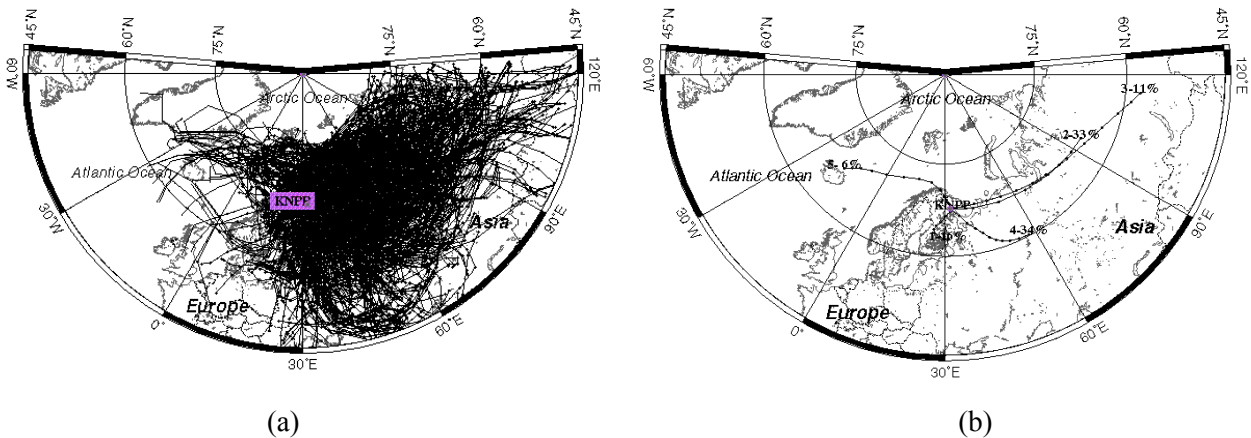


Figure 2.2.1. (a) Isentropic 5-day forward trajectories originated over the Kola NPP region during 1992, and (b) Atmospheric transport pathways from the Kola NPP region during 1992 as a result of trajectory cluster analysis.

For example, Fig. 2.2.1a shows the plotted 5-day trajectories originated during 1992 over the selected site region (Kola nuclear power plant, at the Kola Peninsula). The result of cluster analysis of these trajectories is shown in Fig. 2.2.1b.

It should be noted that in such analysis, the similarity among trajectories in each cluster is maximized considering the full length of each forward trajectory. Within each cluster, individual trajectories can be averaged to obtain the mean cluster trajectory (or atmospheric transport pathway). Thus, the original large data set of trajectories can be reduced to a small number of mean cluster plots. These plots then can be interpreted, based on common synoptic conditions and features, and hence, the airflow climatology for the site can be summarized.

2.3. PROBABILITY FIELDS ANALYSIS OF TRAJECTORY MODELLING RESULTS

Probabilistic analysis is one of the ways to estimate the likelihood of occurrence of one or more phenomena or events. For each site a large number of forward trajectories that passed over various geographical regions were calculated. Each calculated trajectory contains information about longitude, latitude, altitude, pressure, temperature, relative humidity, etc. at each modelling time interval (in this study - 12 hours). The probability fields for these mentioned characteristics, either individual or combined, can be represented by a superposition of probabilities for air parcels reaching each grid area in the chosen domain or on a geographical map.

Let us consider several common approaches to construct probability fields based on trajectory modelling results (*Baklanov & Mahura, 2001; Mahura, 2001; Mahura & Baklanov, 2002*). For all approaches, initially, a gridded domain having $M_{lat} \times M_{lon}$ latitude vs. longitude grid points with a size of $\Delta Y \times \Delta X$ degrees latitude vs. longitude should be constructed. The selection of sizes ΔY and ΔX depends on the resolution of original meteorological fields used for calculation of trajectories. The number of latitudinal and longitudinal grid points - M_{lat} and M_{lon} - is selected taking into account the farthest geographical boundaries which might be reached by air masses during the period studied. Time t is the output modelling time interval which is equal 12 hours for our study.

The first approach to construct such fields considers the number of trajectory intersections with each cell of the gridded domain ($N_{CELL_{ij}}$):

$$N_{CELL_{ij}} = \sum_{k=1}^{N_{tr}} \sum_{j=1}^{M_{lat}} \sum_{i=1}^{M_{lon}} n_{ijk} \quad ,$$

$$n_{ijk} = \begin{cases} 0 \\ 1 \end{cases} \quad \text{if} \quad \begin{cases} X_i \leq X_{k,t} < X_{i+1} \\ Y_j \leq Y_{k,t} < Y_{j+1} \end{cases} \quad ,$$

where:

- $Y_{k,t}, X_{k,t}$ - longitude and latitude of k -trajectory at time t ;
- X_i, X_{i+1} - longitudinal boundaries of the grid cells of the gridded domain;
- Y_j, Y_{j+1} - latitudinal boundaries of the grid cells of the gridded domain;
- N_{tr} - total number of trajectories during the period studied (number of days considered * 8 trajectories per day);
- M_{lat}, M_{lon} - number of the grid points in domain along latitude and longitude.

Examples, given in Fig 3.2.1ab, show the first type of the probability fields: isolines with number of trajectories underline the number of passages by trajectories over the territories. The close to the site the isoline is located, when the larger the number of trajectory passages. The shape of isoline is dependent on the dominating atmospheric transport patterns.

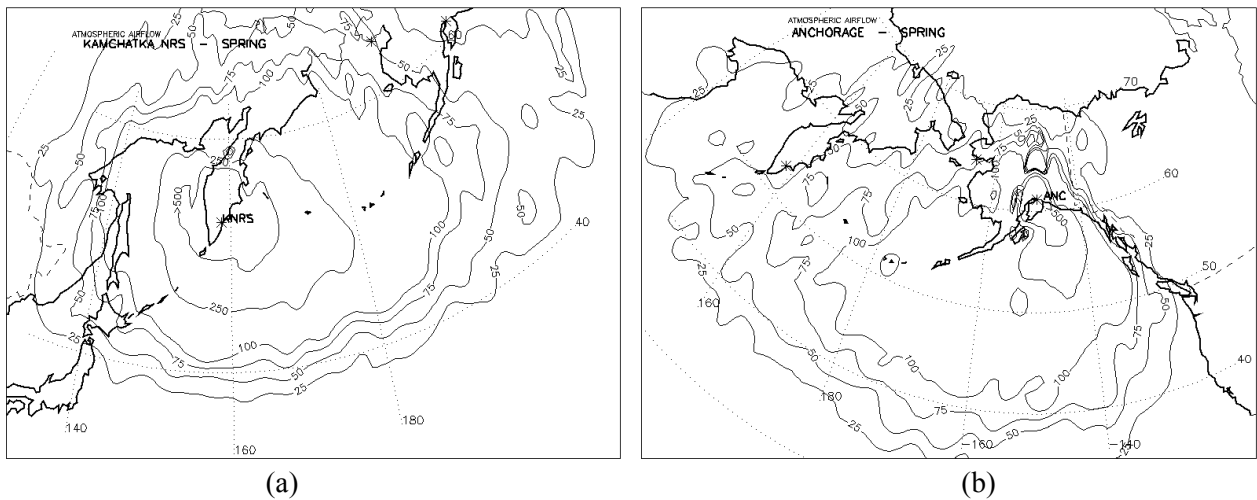


Figure 2.3.1. First type of airflow fields for the: a) source (Kamchatka NRS, Russia) and b) receptor (Anchorage, Alaska) points.

The second approach for construction of probabilistic fields uses an assumption that the total sum of contributions from all individual grid cells of domain is equal to 100%. Hence, the contribution or probability that a given trajectory might reach the geographical boundaries of the individual cell could be estimated as follows:

$$P_{i,j} = \frac{N_{CELL_{ij}}}{N_{tot}} \cdot 100\%,$$

$$N_{tot} = \sum_{i=1}^{M_{lat}} \sum_{j=1}^{M_{lon}} N_{CELL_{i,j}},$$

where:

$P_{i,j}$ - probability of trajectory intersections with a particular cell of the gridded domain;
 N_{tot} - total number of trajectory intersections with all cells of the gridded domain.

Examples, given in Fig 3.2.2ab, show the second type of the probability fields: isolines with percentage of trajectories from the total calculated number of trajectories underline the percentage of passages by trajectories over the territories.

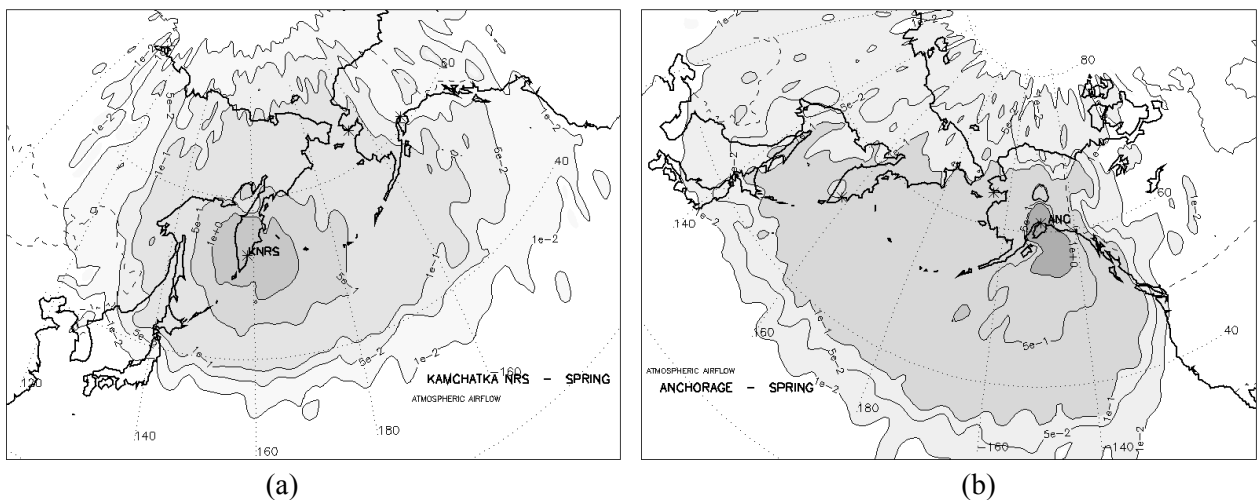


Figure 2.3.2. Second type of airflow fields for the: a) source (Kamchatka NRS, Russia) and b) receptor (Anchorage, Alaska) points.

The third approach for construction of probabilistic fields uses an assumption that for an individual site there is always a region where there is the highest probability of the maximum possible impact due to atmospheric transport. The borders of such region (or more precisely, the cells included in such region) could be estimated by comparing the number of trajectory intersections with the cells (adjacent to the site location) with the cell where the maximum number of intersections occurred: $N_{AMC} = \max\{N_{CELL_{1,1}}, \dots, N_{CELL_{M_{lat}, M_{lon}}}\}$. Among all grid cells, the cell where the absolute maximum of intersections occurred would be identified as an “absolute maximum cell” (AMC). Because all trajectories start near the site region, to account for the contribution into the flow at larger distances from the site, the area of maximum to cells adjacent to the AMC was extended. The number of intersections in cells adjacent to AMC was compared, and then assigned additional cells, which had difference of less than 10% between cells. Therefore, this new “area of maxima”, if isolines are drawn, will represent the area of the highest probability of the possible impact (AHPPI) from the site. Assuming a value of 100% for this area, the rest could be re-calculated as percentage of the area at the highest probability of the possible impact, or:

$$P_{AHPMI_{i,j}} = \frac{N_{CELL_{ij}}}{N_D} \cdot 100\% ,$$

$$N_D = N_{tot} - N_{AHPMI} ,$$

$$N_{AHPMI} = \sum_{j=1}^{M_{lat}} \sum_{i=1}^{M_{lon}} n_{ij} ,$$

$$n_{ij} = \begin{cases} 0 \\ N_{CELL_{i,j}} \end{cases} \quad \text{if} \quad N_{CELL_{i,j}} \geq 0.9 \cdot N_{AMC} ,$$

where:

$P_{AHPMI_{i,j}}$ - probability of the NRS impact with respect to the area of the highest probability of the possible impact (AHPPI) of the site;

N_D - total sum of trajectory intersections with cells from the gridded domain, except the cells located in the boundaries of AHPPI for the site;

N_{AHPMI} – total sum of trajectory intersections with cells from the gridded domain located within the boundaries of AHPPI for the site.

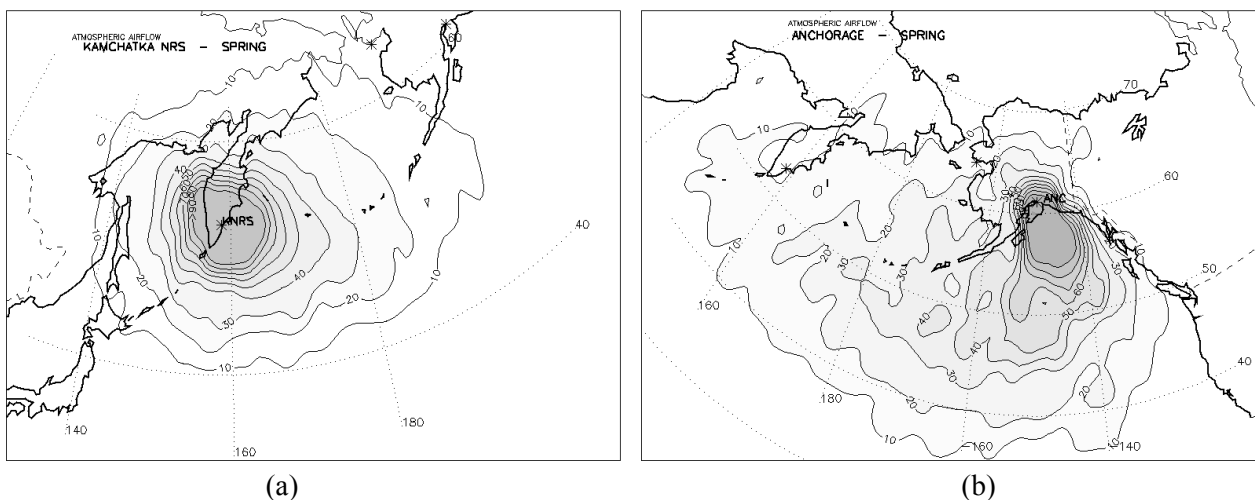


Figure 2.3.3. Third type of airflow fields for the: a) source (Kamchatka NRS, Russia) and b) receptor (Anchorage, Alaska) points.

For example, as shown in Fig. 3.2.3ab, the isolines start from “10” (%) and show contribution of cells into the total redistribution of the airflow around the site with respect to AHPPI. The boundaries of AHPPI are outlined by the isoline of “>90” (%). These both fields showed dominance of the westerly flows from/to the source (Kamchatka) and receptor (Anchorage) sites.

Depending on the considered duration of trajectories it is possible to construct the probability fields for the required terms. If the general atmospheric transport patterns from/to site or region are investigated than the airflow probability fields could be constructed based on the long-duration trajectories, for example, 5 and 10 days. The latter (10-day trajectories) is more valuable if variability of geographical boundaries of the potential remote source/receptor regions are under investigation. In construction of such fields the entire path of trajectories is considered – i.e. trajectory locations at every selected time interval during atmospheric transport. Such examples are shown in Fig. 2.3.4ab for the source (nuclear risk site) and receptor (most populated city of the State of Alaska) points.

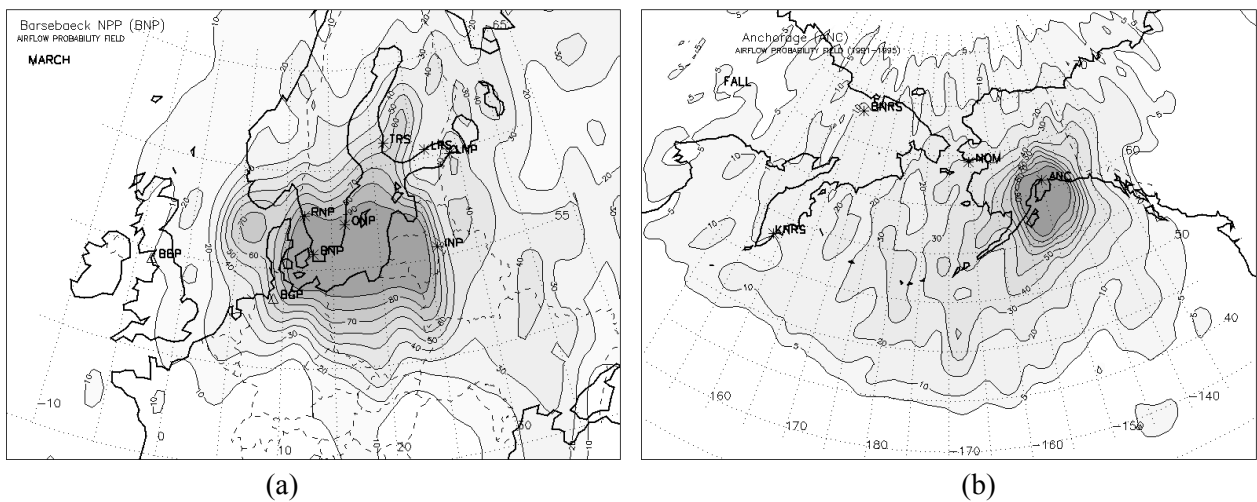


Figure 2.3.4. Examples of the airflow probability fields for the: a) source (Barsebaeck NPP, Sweden) and b) receptor (Anchorage, Alaska) points.

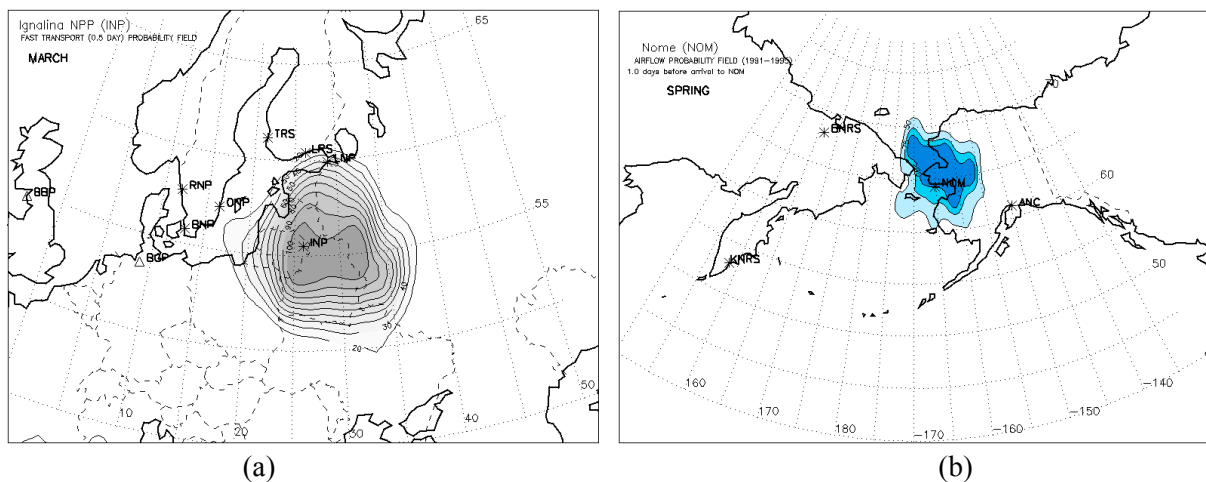


Figure 2.3.5. Examples of the fast transport probability fields for the: a) source (Ignalina NPP, Lithuania) and b) receptor (Nome, Alaska) points.

If the cases of potential accidental releases of hazardous material from the sites occurred or elevated concentration of dangerous pollutants was measured at the monitoring stations, than the

probability fields for the shorter time periods or at the exact terms are valuable. In construction of such fields the endpoints of trajectory paths at selected terms are considered – i.e. trajectory locations at exact time interval during atmospheric transport. These examples are shown in Fig. 2.3.5ab for the source (nuclear power plant in Lithuania, 0.5 days) and receptor (Nome - one of the populated cities of the State of Alaska, 1 day) points.

III. RESULTS AND DISCUSSION

Several approaches in analysis of atmospheric trajectories for identification of the source-receptor relationship will be considered in this section of report. First simple approach is the use of individual and combined forward and backward trajectories (as a result of trajectory modelling of individual and multi-year trajectories). Second approach is the use of individual and combined atmospheric transport pathways from/ to sites and regions (as a result of cluster analysis of atmospheric trajectories for a long-term period). Third approach is the use of individual and combined probabilistic fields (as a result of probability fields analyses of atmospheric trajectories for a long-term period). It should be noted that results of trajectory modelling and their statistical analyses, shown in this report, were used accumulated from different studies performed during 1995-2003.

3.1. USING INDIVIDUAL BACKWARD/ FORWARD TRAJECTORIES TO IDENTIFY POTENTIAL SOURCE/ RECEPTOR REGIONS FOR RECEPTOR/ SOURCE POINTS

The simplest way to identify a potential source region for the specific dates (when an elevated concentration of a particular pollutant was observed) is to calculate backward trajectory/ trajectories arriving at the receptor point at the altitudes of measurements/ observations. Such individual trajectory can be used as an indicator of 1) existence of potential geographical source region with its approximate boundaries, 2) travel time from the potential source region, 3) spatial variations during atmospheric transport when reactions of different nature might have different contribution.

Similarly, the simplest way to identify a potential receptor region for the specific dates (when a hypothetical or real accidents of nuclear, chemical, biological danger occurred at known locations of risk sites or sites of concern) is to calculate forward trajectory/ trajectories originating and departing from the source point at the altitudes of releases. Such individual trajectory can be used as an indicator of 1) existence of potential geographical receptor region with its approximate boundaries, 2) travel time to the potential receptor region, 3) spatial variations during atmospheric transport when reactions of different nature might have different contribution.

Specific Dates with Consistent Airflow to Receptor Points

Let us consider several specific dates (or cases) when the elevated concentrations of pollutants (including CO, CO₂, aerosols, etc.) were recorded at Guam (*Jaffe et al., 1997b*). For these dates, to locate the original possible source regions we calculated individual trajectories (as shown in Fig. 3.1.1) arrived at Guam at dates when the higher concentration of pollutant was observed. The Fig. 3.1.1a shows that the source region is located in the northern latitudes. It represents a possible latitudinal transport of the polluted air mass across the North Pacific Ocean from the free troposphere in the northern latitudes (descending trajectories toward the equatorial zone). The Fig. 3.1.1b shows transport from the east. The origin of trajectories is in the middle of the North Pacific region over the oceanic surface. The atmospheric transport occurred within the lower troposphere,

and it is a relatively slow transport. Although there is no direct source of industrial pollution in this area, we can suggest a possible explanation as the following. First, it is a redistributed polluted air mass arrived from the Asian continent (spring, and in particular, April, is known as one of the months of the relatively fast transport toward the North America continent). Second, there might be a possibility that the natural sources which are active in this region during spring (sea salt particles, DMS). The Fig. 3.1.1c shows almost a direct transport from the west along the intertropical convergence zone (ITCZ). For this case, the transport is observed within the boundary layer. The elevated concentration, recorded at Guam, can be attributed to the burning season on the Indochina Peninsula and adjacent islands of Borneo, Java, and others. In particular, it is associated with the agricultural activities and forest fires during the fall season.

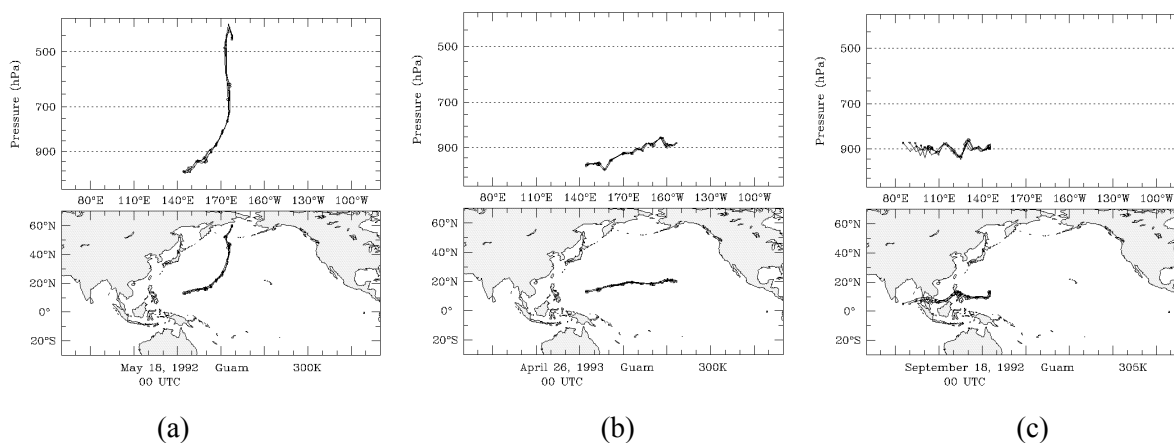


Figure 3.1.1. Isentropic backward trajectories arrived at Guam and showed airflow convergence.

Finally, we should note that all these backward trajectories showed the consistent air flow and converged. Therefore, we clearly can say about the potential geographical source regions from which the polluted air mass arrived and brought elevated concentrations of pollutants. But, it is not always a case.

Specific Dates with Inconsistent Airflow to Receptor Points

Let us consider several specific dates, as shown in Fig. 3.1.2, when the elevated concentration of pollutant was observed at the site.

The Fig. 3.1.2a shows a consistent airflow only during the first several days before arrival at Guam. Although geographically there is an expansion of the possible source region boundaries as well as altitudinal boundaries, we still can associate the elevated concentration at the receptor point (Guam) with the transport from the Asian industrial sources on the seashore of China. The Fig. 3.1.2b shows a more complex structure. The atmospheric transport observed from a wider sector of the Asian continent and also, possibly, from the industrial sources in the southern parts – Ural and West Siberia - of the Former Soviet Union (FSU). The altitudinal variation had increased too – from the boundary layer to the free-flow troposphere. The Fig. 3.1.2c shows an extreme example. The trajectories showing a strong divergence of the air flow arrived at Guam. For this case, the elevated concentration might be associated with the atmospheric transport from the opposite directions – west (continental transport from Asia) and east (maritime transport from the Central North Pacific ocean), i.e. from different potential source regions. Therefore, we can conclude that usage of only one trajectory (as mostly studies employed due to computational expenses) for interpretation of the

elevated concentration of various species at the receptor points vs. possible geographical source regions (associated with source points) is not sufficient. The calculation of several trajectories simultaneously at one altitude as well as at several altitudes will be required, and it is the most correct and useful approach for the specific dates (or cases) studies compared with only one trajectory calculation.

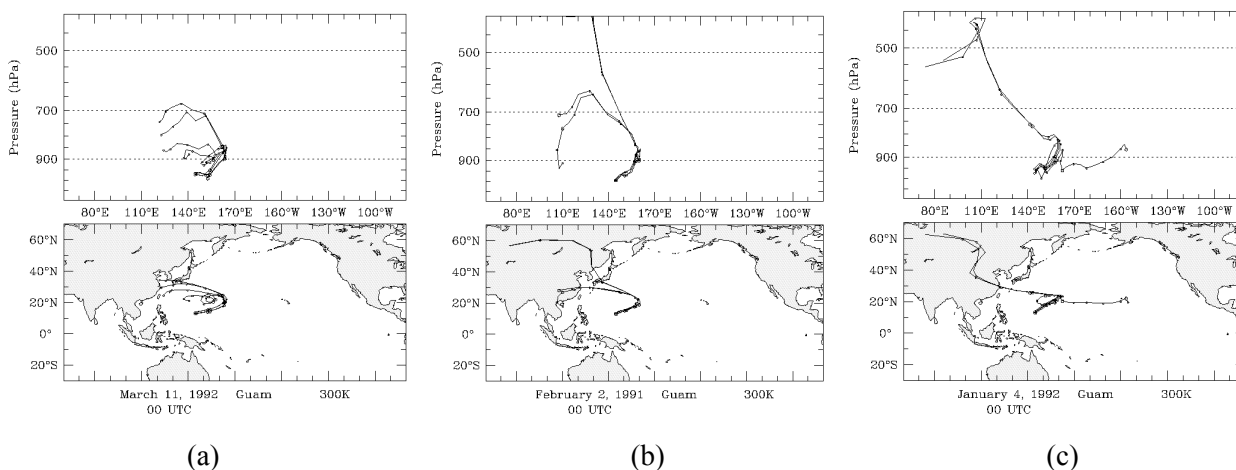


Figure 3.1.2. Isentropic backward trajectories arrived at Guam and showed airflow divergence.

Specific Dates with Consistent Airflow from Source Points

Similarly, the individual forward trajectories can be used to identify the potential receptor regions if they originated over the known source points/ sites. Let us consider several specific dates (or cases) when the hypothetical accidental releases occurred at risk sites. For these dates, to locate the potential receptor regions we calculated individual forward trajectories (as shown in Fig. 3.1.3). The Fig. 3.1.3a shows that for the Loviisa NPP (Finland) the boundaries of the receptor region are located to the east of the site along the 45-60°N latitudinal belt. For the boundary layer transport the receptor region is in the central part of Russia; for the free troposphere transport (which occurred after several days) – over the Ural mountains.

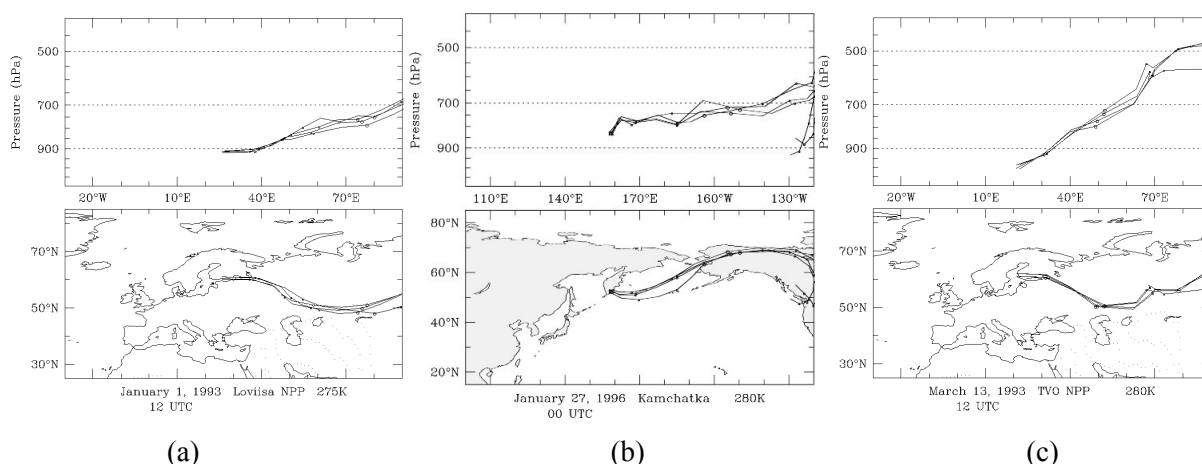


Figure 3.1.3. Isentropic forward trajectories originated at the a) Loviisa NPP, Finland, b) Kamchatka site, Russia, c) Olkiluoto (TVO) NPP, Finland and showed airflow convergence.

The Fig. 3.1.1b shows trajectories originated over the Kamchatka site (Russian Far East). The potential receptor regions for this site are located along 20 degrees latitudinal belt (50-70°N). Two

potential receptor regions should be considered. The first region, after a first few days of released radioactivity cloud motion within the boundary layer from the site, is an interior of the State of Alaska. The second region is over the western seashore of North America (industrialized populated regions and counties on the shore of the Pacific Ocean). As seen from this figure, the air mass did not pass the Rocky mountains and it descended down the mountain slopes to the surface. The Fig. 3.1.3c, similarly to the Loviisa site, showed the same receptor regions for the Olkiluoto (TVO, Finland) nuclear plant, although the receptor region over the Ural mountains is located higher by altitude – in the middle troposphere ($\approx 4-5$ km).

Specific Dates with Inconsistent Airflow from Source Points

Let us consider several specific dates (or cases) when the hypothetical accidental releases of radioactivity occurred at the risk sites, but during atmospheric transport the trajectories showed a significant divergence of flow. For these dates, to locate the potential receptor regions we calculated individual forward trajectories (as shown in Fig. 3.1.4).

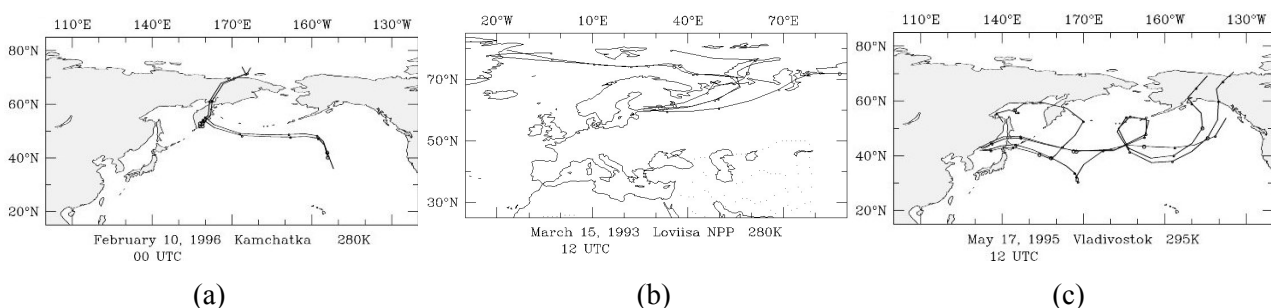


Figure 3.1.4. Isentropic forward trajectories originated at a) Kamchatka NRS, Russia, b) Loviisa NPP, Finland, c) Vladivostok NRS, Russia and showed airflow divergence.

As for the specific dates when airflow was consistent, and hence, the potential receptor regions were situated along the path of trajectories, the dates shown in Fig. 3.1.4 have another peculiarity – the receptor regions can be situated even in the opposite directions. The Fig. 3.1.4a shows that there are two potential receptor regions for the hypothetical release occurred at the Kamchatka site at 10 Feb 1996, 00 UTC. One of the regions is to the north of the site (2000-2500 km, Arctic seashore of Russia). Other region is to the east of the site (5000-5500 km, over the eastern part of the North Pacific Ocean). The Fig. 3.1.4b shows that there are also two distant potential receptor regions located in the opposite directions from the Loviisa NPP. Although both receptor regions are located within the Arctic latitudes: the first is over the Greenland and surrounding Arctic seas (to the west of the plant), the second is over the Russian Arctic (to the east of the site). Moreover, during the first few days the receptor region on a regional scale is the Northwest Russia. The Fig. 3.1.4c shows that there are also several receptor regions for the hypothetical release at the Vladivostok site at 17 May 1995, 12 UTC. The first region (relatively closely located, on a range of 1500 km from the site) is situated over the Magadan and Kamchatka regions and Okhotsk Sea. Two others are more distant regions. The first of these two is over the belt of the Aleutian Chan Islands (5000-6000 km to the east of the site). The second region is over the Gulf of Alaska, southern territories of the State of Alaska, and the Canadian Arctic (8000-10000 km to the east of the site).

As we seen, the individual trajectories sometimes can be successfully used when specific cases are considered, although in situations of airflow strong divergence during atmospheric transport from/to sites the trajectories became more “questionable and confusing” for clear identification of sources and receptors for pollutants.

For individual trajectories used in interpretation of source-receptor relationship there is a problem related to a question: *What occurs when a longer period of multiple trajectories is considered?* Does it change an identification of the source-receptor relationship for atmospheric pollutants? Hence, let's us consider another approach to extract this “when” information.

3.2. CLUSTERING OF BACKWARD TRAJECTORIES TO IDENTIFY POTENTIAL SOURCE REGIONS FOR RECEPTOR POINTS

The cluster analysis of trajectories both backward and forward for the long-term periods of time in the atmospheric sciences is one of the most useful tools to identify the general airflow patterns, including average transport times and probabilities of transport, within meteorological systems. Cluster analysis of forward trajectories allows identification of the common atmospheric transport pathways from a selected site (source point). Cluster analysis of backward trajectories allows identification of the common atmospheric transport pathways to a selected site (receptor point).

Cluster Analysis for Identification of Atmospheric Transport Pathways to Receptor Points

The Fig. 3.2.1 shows cluster analysis results for two receptor points – Nome and Shemya - located in Alaska. For clustering, we used a multiyear (1991-1995) dataset of backward trajectories arrived at both sites. Therefore, the general atmospheric transport pathways to the selected sites are the average annual characteristics. The specificity in the selection of the number of clusters was related to project purpose to identify a cluster, which is located as closer as possible to the source point, i.e. the Bilibino NPP region (*Mahura et al., 1997*). For Nome (Fig. 3.2.1a), we identified 6 clusters or atmospheric transport pathways to the site. Three clusters (#2, 3, and 5) showed transport from the west and occur in total 49% of the time.

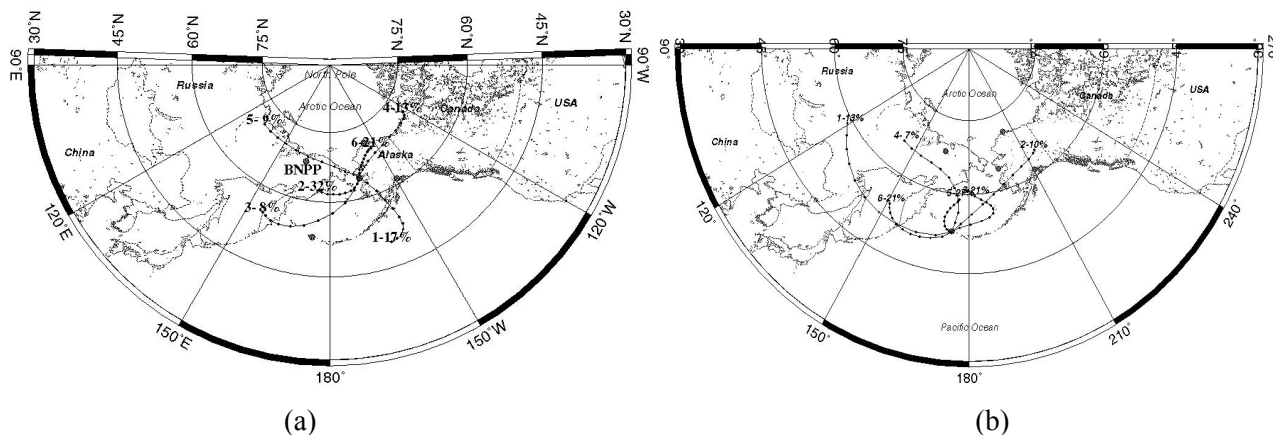


Figure 3.2.1. Atmospheric transport pathways to receptor points in Alaska: a) Nome and b) Shemya.

The cluster #1 (17% of the time) represented transport from the south. Two other clusters (#4, 6) showed transport from the Northern Arctic latitudes of Alaska (21%) and Canadian Arctic (13%). The cluster #5 (9%) is the closest located to the Bilibino NPP (source point) region. Therefore, we can conclude that on an annual basis the probability of atmospheric transport to Nome (receptor point) is 9% of the time, and on average it can take of 2.5 days. A similar interpretation could be done for Shemya (Fig. 3.2.1b), where we identified on an annual basis 7 clusters or atmospheric transport pathways to the site. There is no cluster located closely to the

Bilibino NPP region compared with Nome, although we still might assume that such possibility could exist. We know, that in the cluster analysis output and visualization some information between clusters is missing, and therefore, another type of analysis would be required to avoid this information gap (see §3.5).

We should note that the trajectory curvature of each of the transport pathway (or mean cluster trajectory) is a good indicator of the cyclonic or anticyclonic circulation in the airflow. For example, as shown in Fig. 3.2.1a, the cluster #3 is an indicator of the cyclonic circulation, i.e. the air mass would be moving in the anticlockwise direction. In opposite case, as shown in Fig. 3.2.1b, the cluster #3 is an indicator of the anticyclonic circulation, i.e. the air mass would be moving in the clockwise direction. Additionally, we should note that for the sites (for example, such as Shemya) located in the areas of the high atmospheric activities (for example, the Aleutian Low) the calculated trajectories have a complex structure. Shemya is located along the main track of cyclones moving toward north-eastern direction as well as the Bering Sea area is well known as an area for the stagnation of cyclones. Therefore, the clustering of trajectories outlined a complex structure of the atmospheric transport pathways for this site as shown in Fig. 3.2.1b.

Cluster Analysis for Trajectories of Different Duration

The trajectories of longer duration (more than 5 days) experienced problems in quality of calculation, and hence, are less reliable. Although we should note, that for specific dates studies, especially, related to identification of the source regions the longer duration of trajectory is a better choice. Let us consider differences in clustering of 5 vs. 10 day backward trajectories. For this purpose, we will use trajectories for the Guam specific dates during 1989-1994 (Fig. 3.2.2). In particular, all these trajectories – for 87 specific dates - showed elevated concentration of CO₂ at the Guam measurement site (*Jaffe et al., 1997b*). The difference between 5 and 10 day trajectories is only that for 5 day trajectories the same dataset of trajectories was resorted, i.e. all trajectories were terminated exactly at 5 days of transport as well as at 10 days of transport.

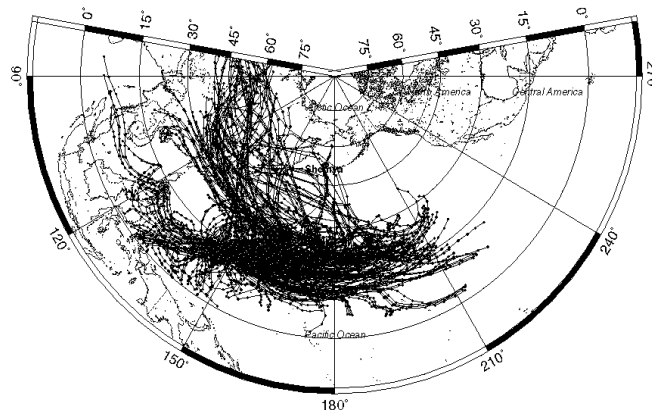


Figure 3.2.2. Isentropic backward trajectories arrived at Guam for the selected specific dates during 1989-1994.

The results of clustering (*Mahura & Jaffe, 1998*) are shown in Fig. 3.2.3. For the specific dates, the clustering of 5 days trajectories showed (Fig. 3.2.3a) 6 clusters. The major transport to Guam occurred from the eastern direction – clusters #3 and 5 with 40 and 35% of the time, respectively – the Central North Pacific region. The slow atmospheric transport from the west – cluster #2 (15% of the time) – is associated with the transport from the equatorial band islands of

Borneo, Java, and others. The transport from continental territories of Asian occurred 8% of the time, and from the southern remote areas of FSU – only 2% of the time.

The cluster analysis of 10 days trajectories arrived at Guam for the same specific dates showed also the dominance of the atmospheric transport from the east – 66% of the time (as shown in Fig. 3.2.3b). Transport from the Asian sector occurred 34% of the time, where the Indochina region contributed only 6%, and the rest is from the seashore (23%) and continental (5%) parts of Asia. Based on this analysis we can conclude that, in general, there is a difference in results of the cluster analysis for trajectories of different duration, although the presence of the major transport patterns remained the same, for example, as dominance of transport from the east to Guam. It seems more valuable to use for identification of the source regions for the receptor points the trajectories of longer duration (in order to account more distant source regions with respect to the receptor points), although there is a factor of uncertainty due to quality of trajectory calculation.

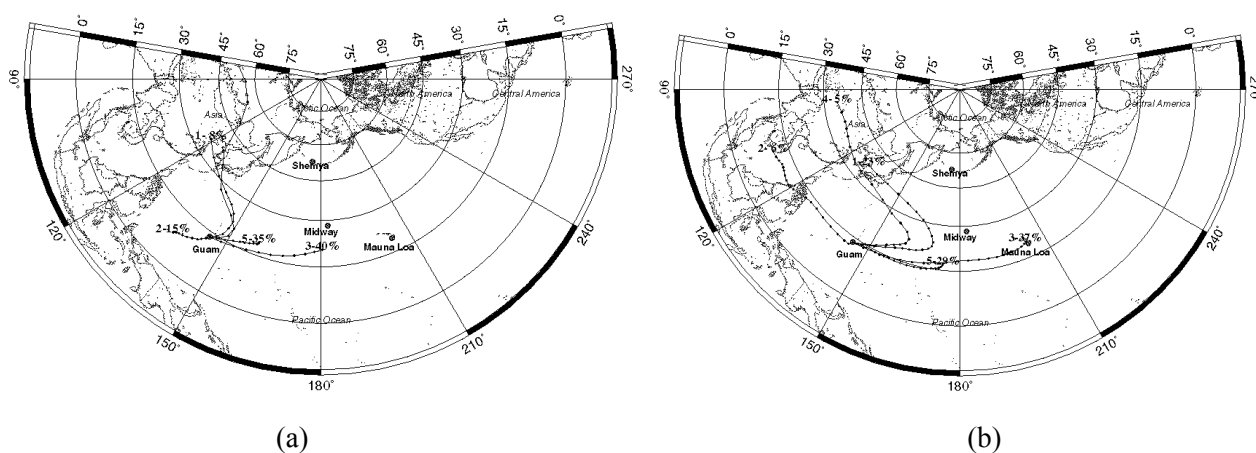


Figure 3.2.3. Atmospheric transport pathways to Guam based on clustering of a) 5 days and b) 10 days isentropic trajectories.

Approaches in Grouping of Trajectories

Several approaches can be selected for the trajectory grouping. First approach is a grouping of trajectories on a temporal scale. The second is an altitudinal grouping of trajectories.

We should note that the annual atmospheric transport pathways, based on a multiyear dataset, is useful information, although a separation of trajectories into smaller “temporal” groups – by year, season, month, UTC term, etc. - can provide more detailed information. For example, let us consider a seasonal variability for the same Guam’s specific cases (*Mahura & Jaffe, 1998*). The trajectories for these specific dates (sorted by season) are shown in Fig. 3.2.4.

The visual inspection showed that summer-fall had the lowest number of cases attributed to the continental Asia sources, and when the elevated concentrations were observed at Guam. The fall represented the increased number of transport (southerly of 15°N) from the Indochina region and equatorial islands due to agricultural burning and forest fires. During winter-spring, most of the time the atmospheric transport occurred from the Central North Pacific region, although occasionally there are cases of transport from the Asian source located northerly of 15°N. Observing a seasonal variation in identification of the source regions for trajectories, it seems reasonable that the cluster analysis of trajectories by season will provide more representative information about variations in the occurrence of the specific dates at Guam.

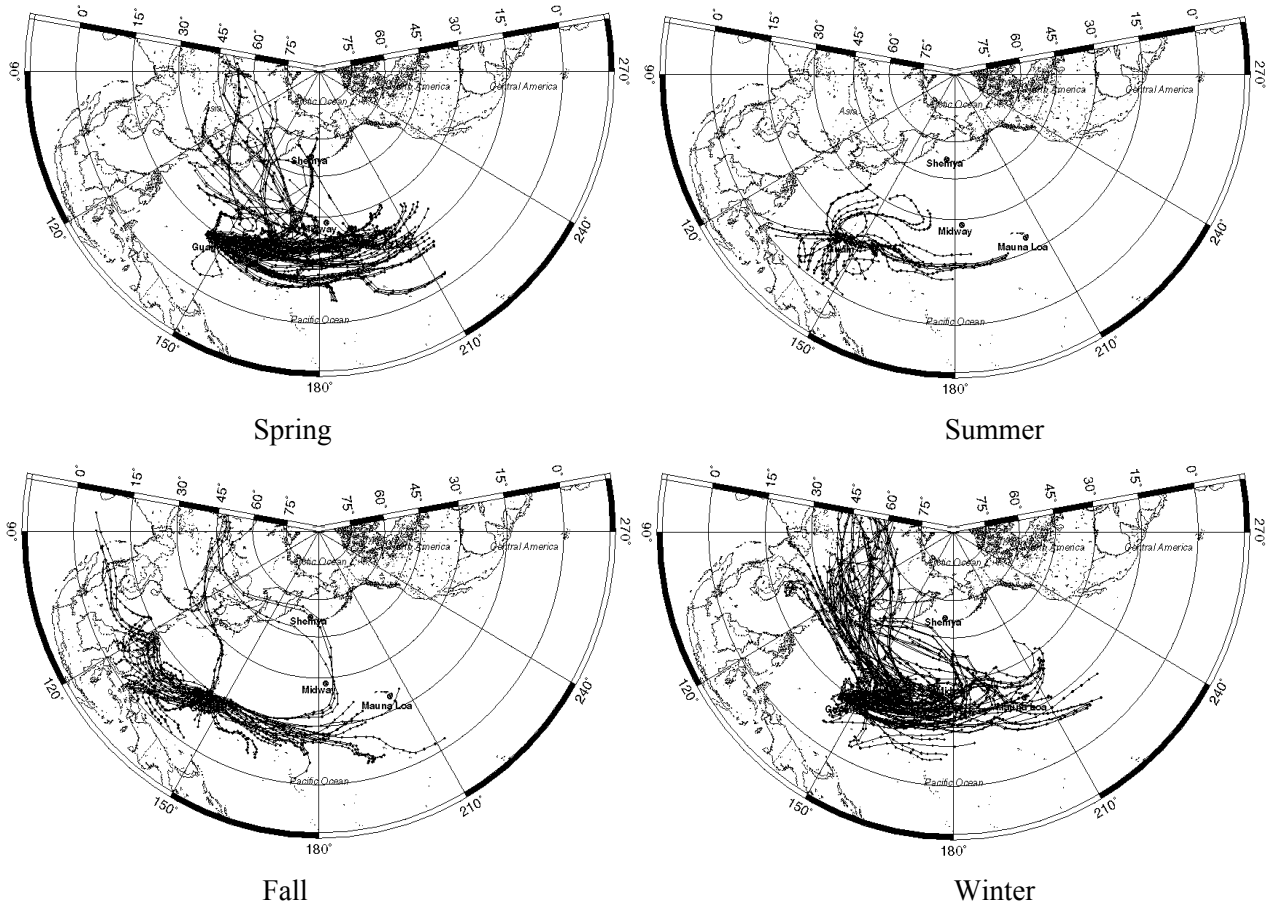


Figure 3.2.4. Isentropic backward trajectories arrived at Guam by season (for the selected specific dates during 1989-1994).

Altitudinal Variations of Trajectories

To evaluate the airflow patterns variability it is important to consider also the altitudinal variation of trajectories. For these purposes, it would be useful to calculate trajectories at several altitudes. For example, as shown in Figs. 3.2.5abc, we plotted all 10-day backward trajectories arrived at Barrow, Alaska during 1985 at three altitudes of 500, 1500, and 3000 m above sea level (asl). These altitudes represent transports within the boundary layer, boundary region between the boundary layer and free troposphere, and free troposphere. The trajectories were plotted to identify the frequency of atmospheric transport from several potential source regions (European and Taymyr, Canadian Arctic, and 3 regions of the North Pacific) for atmospheric pollutants. As shown on these figures, there is a significant extension of trajectory coverage/passage over the source regions with an increasing of altitude. The origin of trajectories arrived at Barrow is also located more farther from the site with an increasing of altitude, but the transport time decreased (except for the Canadian Arctic region due to its proximity to Barrow) as shown in Tab. 3.2.1. Moreover, the variability of trajectories at three altitudes vs. source regions were investigated by *Mahura et al., 2003b* and showed some peculiarities (Tab. 3.2.1).

The number of trajectories passing over several regions simultaneously (MT category) increased by 3 times at 3 km compared with 0.5 km altitude. The atmospheric transport from the Pacific (NP1, NP2, and NP3) and European (ER) regions increased with an increasing of altitude. Number of trajectories from the Canadian Arctic (CA) and Taymyr (TR) regions decreased with

altitude increased. But atmospheric transport from these two regions is still remained as dominating pattern compared with other source regions.

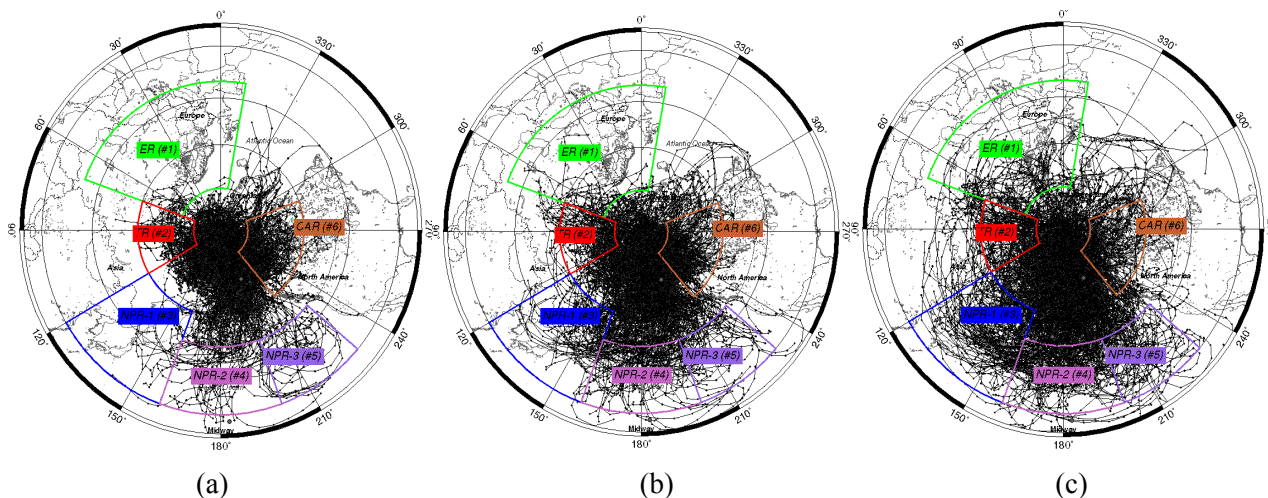


Figure 3.2.5. Isentropic backward trajectories arrived at Barrow, Alaska during 1985 at altitudes of a) 500 m, b) 1500 m, and c) 3000 m.

Table 3.2.1. Transport patterns for Barrow at different altitudes vs. source regions.

Region vs. Altitude (km)	No Source	European ER	Taymyr TR	West North Pacific NP1	Central North Pacific NP2	East North Pacific NP3	Canadian Arctic CA	Mixed Trajectories MT
Annual average and interannual range of distribution of trajectories (in %)								
0.5	27.5 (23.4-33.7)	1.2 (0-2.6)	11.2 (5.9-16.8)	1.6 (0.3-3.6)	3.6 (1.8-5.5)	2.4 (0.9-6.7)	38.2 (26.8-49.2)	14.3 (10.7-17.3)
1.5	21.7 (18.7-27.3)	1.9 (0.1-4.8)	11.8 (7.1-16.8)	4.7 (2.6-7.9)	5.1 (2.3-7.8)	2.8 (1-6.3)	25.9 (16.4-33.1)	26.1 (20.4-30.5)
3.0	14.7 (10.7-20)	3.4 (1-7.8)	8.0 (5.9-9.9)	6.9 (5.3-9.2)	5.6 (4.2-8.1)	3.0 (1.1-5.8)	14.6 (9.6-18.9)	43.7 (37.3-49.6)
Average transport time \pm standard deviation (in days)								
0.5		7.6 \pm 1.6	6.1 \pm 2.1	7.3 \pm 1.7	6.6 \pm 2.1	6.0 \pm 2.2	3.2 \pm 2.5	
1.5		6.8 \pm 2.0	6.1 \pm 2.3	6.5 \pm 2.0	5.8 \pm 2.2	6.0 \pm 2.2	3.2 \pm 2.5	
3.0		6.0 \pm 2.1	6.0 \pm 2.3	5.9 \pm 2.2	5.6 \pm 2.4	5.4 \pm 2.4	3.6 \pm 2.6	

The interannual variability of atmospheric transport to Barrow from regions is large. In some years – there is no any transport or there is very low probability of transport from a region (for example, for the European region at altitudes of 0.5 and 1.5 km). In other years – there is a substantial ten-times and more increase in transport from a region (for example, for the European and North Pacific regions).

3.3. CLUSTERING OF FORWARD TRAJECTORIES TO IDENTIFY POTENTIAL RECEPTOR REGIONS FOR SOURCE POINTS

If a multiyear dataset of trajectories is available than it is possible to identify the general atmospheric transport from the selected points/regions of concern. For example, as shown in Fig. 3.3.1ab, the annual atmospheric transport pathways from the Vladivostok naval base (Russian Far East) (Fig. 3.3.1a) and the nuclear power plant (Fig. 3.3.1b) on the Kola Peninsula of Russia were evaluated employing the cluster analysis technique.

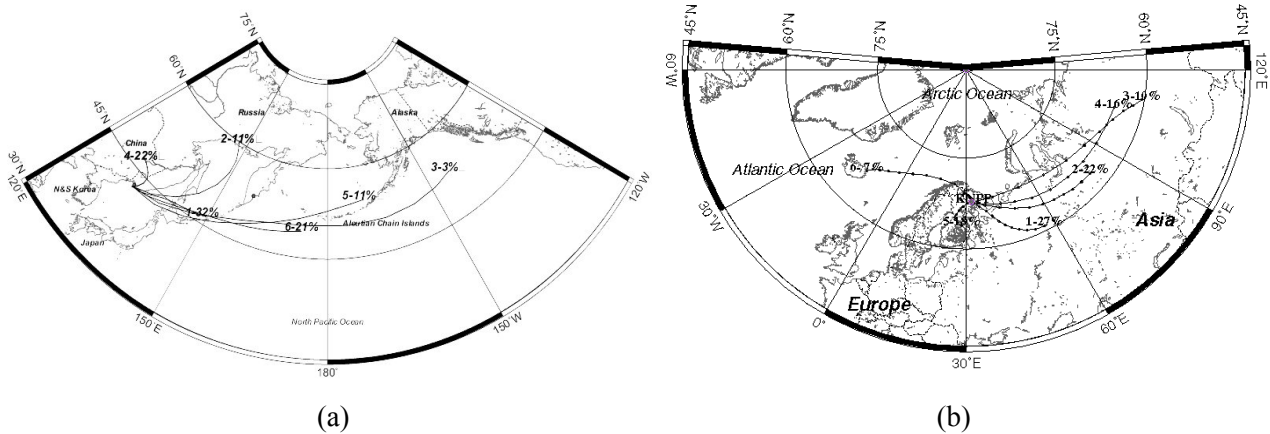


Figure 3.3.1. Annual atmospheric transport pathways for trajectories originated within the boundary layer a) from the Vladivostok naval base (based on 1987-1996 trajectories) and b) from the Kola nuclear power plant (based on 1991-1996 trajectories).

For the Vladivostok naval base, six clusters were identified for the trajectories originating within the boundary layer over the site region (Fig. 3.3.1a). Four of them (#1, 3, 5 and 6 with 32, 3, 11 and 21% of occurrence, respectively) also show westerly flow. These were observed about 67% of the time. Among these clusters, cluster #3 represents the possibility of the relatively rapid westerly flow toward the North America territories. Cluster #4 (22%) shows easterly flow. Cluster #2, which occur 11% of the time, is transport with a northward component of the flow through the Okhotsk Sea. Throughout the year, westerly flow is also dominant for the base region. Transport from the west varies from 68% (in fall) to 82% (in summer) of the time. Transport from the east occurs only during winter-spring and varies from 7% (in spring) to 10% (in winter) of the cases. Transport with the northward component is a peculiarity of the site. It is reflected in each season throughout the year and varies from 14% (in winter) to 32% (in fall) of the time.

For the Kola nuclear power plant, six clusters were identified for the region (Fig. 3.3.1b). Four of them (#1, 2, 3 and 4 with 27, 22, 10 and 16% of occurrence, respectively) show westerly flow. These observed about 75% of the time. Cluster #6 (7%) shows easterly flow toward the Northern Atlantic both within the boundary layer and free troposphere. Cluster #5, which occur 18% of the time, is transport to southwest through the Scandinavian Peninsula into the Baltic Sea. Throughout the year, westerly flow is predominant for the plant region. Transport from the west varies from 68% (in fall) to 94% (in spring) of the time. Transport from the east occurs from 3% (in winter) to 26% (in summer) of the cases. Transport with the southward component take place 15% of the time (in winter) increasing up to 25% (in fall). Analyzing trajectories at the higher altitudes - 1.5 and 3 km asl - we also found that within the free troposphere the probability of transport from west increases up to 90%.

For both sites considered the receptor regions are more likely to be located in the eastern sector from the sites. For the Vladivostok naval base, these are areas of the Japanese Islands and the

Aleutian Chain Islands, US in the North Pacific region (in total, more than 60% of the time air masses could pass over these regions). Moreover, the populated areas of the North-West China and the Magadan region, Russia are also should be considered as receptor regions (accounting for 33% of the potential transport over these regions). For the Kola nuclear power plant, the receptor regions are mostly to the east of the site, although a region over Iceland can be identified.

In both cases, different scales for receptor regions with respect to sources could be seen. First, the receptor regions are situated on the regional scale from the sources. For example, the Japanese Islands, Magadan, and North-West China regions are regions located within several hundreds km range from the naval base (Fig. 3.3.1a). The North-West Russia and some of the Scandinavian countries are also regions located within the same range with respect to the nuclear plant (Fig. 3.3.1b). Second, the receptor regions situated on the large-scale and far remotely from the sources. For example, the Aleutian Chain Islands with respect to the Vladivostok site (Fig. 3.3.1a) and the industrialized Ural and Western Siberia regions of Russia with respect to the nuclear plant (Fig. 3.3.1b).

Such cluster analyses provided brief and crude information about potential geographical receptor regions with respect to sources, although it did not underline and distinguish the boundaries of these regions. Hence, we can only speculatively define the potential geographical boundaries of receptor regions as well as probability of how often atmospheric transport to these regions can occur on different temporal scale (i.e. if annual, seasonal, monthly variability of transport pathways are considered).

3.4. COMBINED ANALYSIS OF FORWARD-BACKWARD TRAJECTORIES FOR IDENTIFICATION OF SOURCE-RECEPTOR RELATIONSHIP

To compare the degree of the dependence of the receptor vs. source point/region, the combined analyses can be performed. Let us consider analyses of source-receptor relationship for two sites located in the North Pacific region.

For the Kamchatka site, serving as a nuclear source, six clusters were identified for the trajectories originating over the site region within the boundary layer (Fig. 3.4.1a). Four of them (#1, 2, 3 and 4 with 2, 31, 8 and 22% of occurrence, respectively) show westerly flow. These were observed about 63% of the time. Cluster #1 was used to show the possibility of the relatively rapid westerly flow toward the State of Alaska and Canadian territories. Cluster #6 (8%) shows easterly flow toward the continent both within the boundary layer and free troposphere. Cluster #5, which occurred 29% of the time, represents transport to the west, but it is significantly slower when compared to cluster #6. Throughout the year, westerly flow is predominant for the site. Transport from the western directions varies from 63% (in winter) to 87% (in spring) of the time. Transport from the eastern directions occurs from 15% (in fall) to 37% (in winter) of the cases. Transport in the northward direction is only apparent during fall, and it is equal to 17% of the cases.

For Anchorage, one of the most populated cities of the State of Alaska and located on the south side of the Alaska Range, most of the transport is from the south and south-west (Fig. 3.4.1b). This situation occurred more than 80% of the time. Clusters (#1, #2, #3, and #5) have a significant cyclonic curvature and correspond with transport by the Aleutian Low. These regions are also the main cyclone pathways. Approximately 8% of the trajectories are in cluster #4, which showed north-easterly flow with a 5-day origin over the Northern Canada and it had an anticyclonic curvature. As seen, in about 13% of the cases the transport is associated from the Kamchatka Peninsula as shown by cluster #5. In about 7% of the cases the transport is associated from another

potential source (Bilibino nuclear power plant, Russia) as shown by cluster #6. Seasonal variability of these patterns is discussed in *Jaffe et al., 1997a* and *Mahura et al., 2002*.

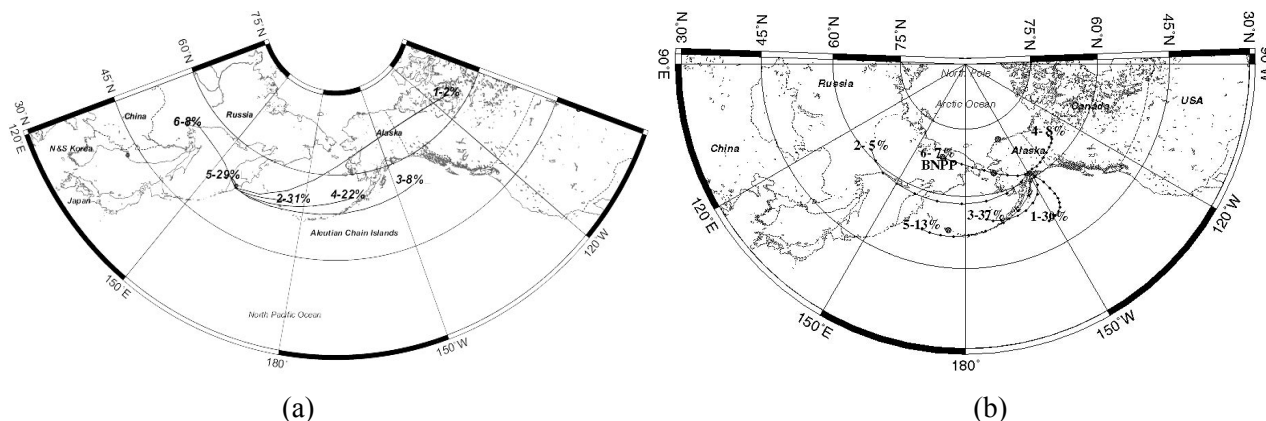


Figure 3.4.1. Annual atmospheric transport pathways for trajectories originated within the boundary layer a) from the Kamchatka site, Russia (based on 1987-1996 trajectories) and b) to Anchorage city, Alaska, US (based on 1991-1995 trajectories).

For the Kamchatka site, the remote populated receptor regions are more likely to be situated within the Russian Far East (less than 10% of transport occurred in this direction) and the State of Alaska, US (more than 60% of transport occurred in that direction) territories. Moreover, approximately 30% showed that the receptor areas are on the local to meso-scales. For Anchorage, all potential source regions are situated farther than a 1000-km range. These are the Kamchatka and Chukotka regions of Russia with the surrounding seas, Canadian Arctic territories, and the Gulf of Alaska. Practically all these source regions, except the Canadian, are located to the west of the site showing the dominating transport by westerlies (92% of the time).

Among all clusters, shown in Fig. 3.4.1, only four for each site were intercepted along the paths of air parcels motion. The transport - along the northern part of the Aleutian Chain Islands and the southern aquatoria of the Bering Sea (1st path) - from the Kamchatka site occurred 53% vs. 50% of the time for air masses arrived at Anchorage. Transport toward/from the Gulf of Alaska (2nd path) occurred 8% vs. 30% of the time for the Kamchatka and Anchorage sites, respectively. Transport over the middle aquatoria of the Bering Sea (3rd path) occurred in less than 5% of the cases. Hence, the most probably atmospheric transport from Kamchatka to Anchorage will be though the first joint path occurred more than 50% of the time for both sites with times of transport ranging from 6 to 8 days. Two others paths are less probable. For the 3rd path the transport times will be – from 4 to 6 days, and for the 2nd path – from 9 to 10 days.

Based on comparison of intersections for atmospheric transport pathways from/to sites of concern (source/ receptor) it is possible: 1) to identify the most probable joint transport pathway for air parcels departing/arriving from/at the sites; 2) to evaluate what is a probability of occurrence of such transport pathway, 4) to calculate how much time (days) it will take for an air mass to travel between two sites, 3) to estimate where (a belt or region of geographical territory) an interception of air masses arriving/departing will occur.

For clustered both forward and backward trajectories used in interpretation of source-receptor relationship there is a problem related to a question: *What occurs between atmospheric transport pathways?* Does it change an identification of the source-receptor relationship for atmospheric pollutants? Hence, let's consider another approach to extract this “**between**” information.

3.5. PROBABILISTIC FIELDS ANALYSIS FOR SOURCE POINTS TO IDENTIFY RECEPTOR REGIONS

Another way to identify more detailed geographical boundaries of potential receptor regions for the source points is use the method of probability fields analysis shown in §2.3. Several examples of such fields are given in Figs. 3.5.1 and 3.5.2. These show the annual airflow probability fields constructed for the risk sites located in the Russian Far East (Fig 3.5.1) and Euro-Arctic (Fig. 3.5.2) regions. All these sites showed an elliptical form of the airflow fields and a significant domination of westerly flows in formation of these fields, although some peculiarities can be seen. For both Arctic latitude sites there is a pattern of the airflow extension in the south-western direction from the sites over the Magadan region and Finnish territories for the Bilibino and Kola sites of the Euro-Arctic region, respectively. Due to influence of the Gulf Stream current, the British site has more stretched field along the NE-SW direction compared with other directions as well as other sites. Similarly, the Vladivostok site, located along the main tracks of cyclonic system of the Aleutian Low, has field also extended in the NE-SW direction.

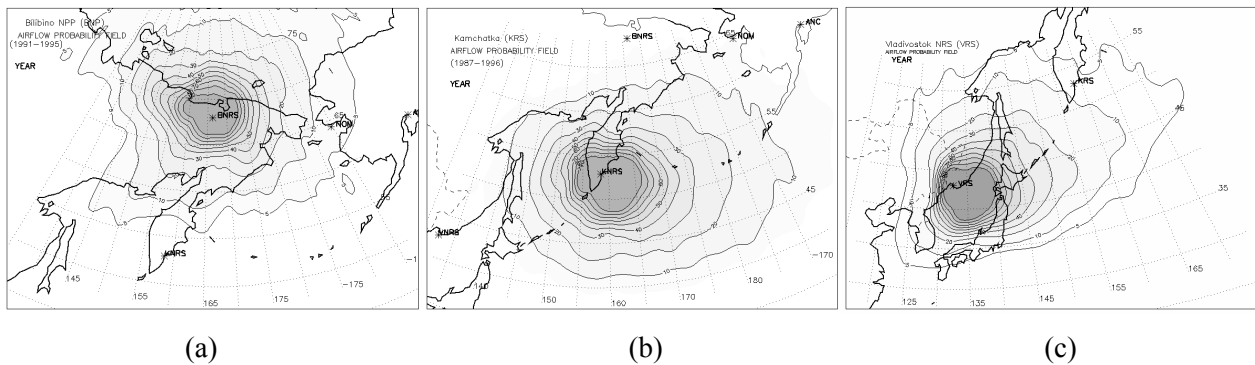


Figure 3.5.1. Annual airflow probability fields for the Russian Far East nuclear risk sites (source points): a) Bilibino NPP, Russia, b) Kamchatka NRS, Russia, and c) Vladivostok NRS, Russia.

All these fields reflect the potential impact (in %) on remote regions with respect to the area where the impact is the highest (i.e. within territories surrounding the site on the local and mesoscales). For example, considering the Bilibino site (Fig. 3.5.1a), one can mention that the probability of impact over the middle and southern territories of the Kamchatka Peninsula will be less than 5% of what can be within the boundaries (>90) of the area where the impact is the highest. In the same time (Fig. 5.3.1b), for the Aleutian Chain Islands (although they are reachable during atmospheric transport from the Kamchatka site) the chances of “being largely hit” by a contaminated radionuclide cloud are lower (from 40 to 10% of potential impact which might be in vicinity of the site) and practically negligible for the populated cities of the State of Alaska. In particular, employing the dispersion modelling approach for specific cases studies, *Mahura et al., 2002* showed that after 5 days of atmospheric transport the radionuclide time integrated air concentration (TIAC), dry deposition (DD), and wet deposition (WD) at most populated Alaskan cities (Anchorage, Fairbanks, Nome, etc.) were lower by 6-8 orders of magnitude compared with emitted amounts at the site. Employing the long-term dispersion modelling approach for the same site it was found that over the studied territories (the Aleutian Chain Islands, State of Alaska, and Bering Sea aquatoria) the TIAC, DD, and WD decreased by 1-2 orders of magnitude. Moreover, all these fields as well as the airflow probability field had a significant seasonal variability.

Considering interrelation between two sites – Kamchatka and Vladivostok – shown in Fig. 3.5.1bc it should be noted that although the Kamchatka site is a potential receptor region for the

Vladivostok site, it is not valid if opposite (i.e. the airflow probability field of the Kamchatka site showed that territories surrounding the Vladivostok region are not reachable, and hence, impact will be negligible).

The source points shown in Fig. 3.5.2 can be separated by geographical locations to the types of the climate regimes observed there. In particular, among 16 NRS considered in the Euro-Arctic region three groups were identified by peculiarities of the climatological airflow patterns, concentration and deposition fields (Mahura *et al.*, 2003d). Among these sites, the Leningrad site shown in Fig. 3.5.2a is an inland type, the British site shown in Fig. 3.5.2b is a maritime type, and the Kola site shown in Fig. 3.5.2c is an Arctic type. Moreover, there is also an intermediate type related to the transport of the maritime/ inland regime. For the Kola and Leningrad sites, the European part of Russia extending to the Ural mountains represents a potential receptor pool. These are the most populated territories, especially the middle latitudes. For the British site, the receptor regions are located in the N-E sector of the site – Scandinavian countries and countries along the seashore of the North and Barents Seas.

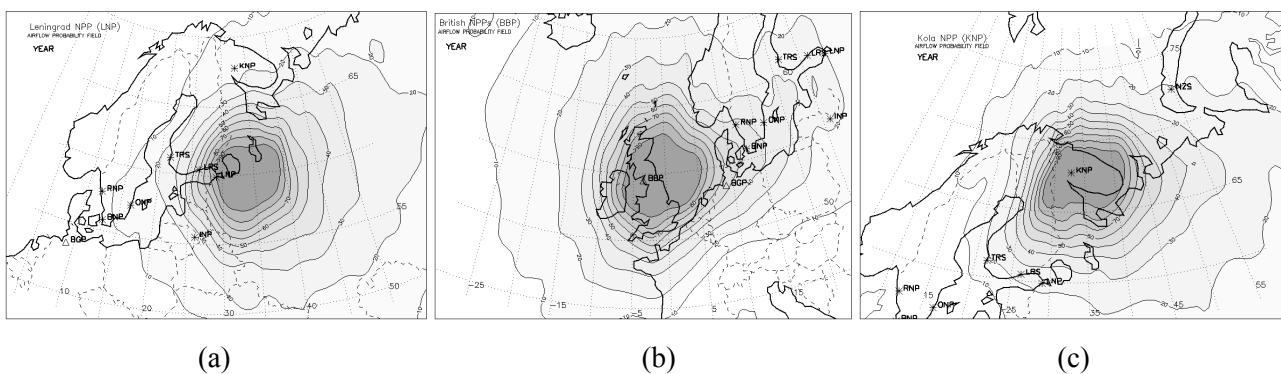


Figure 3.5.2. Annual airflow probability fields for the European nuclear risk sites (source points): a) Leningrad NPP, Russia, b) Block of the British NPPs, UK, and c) Kola NPP, Russia.

Moreover, in addition to the airflow probability fields (which are mostly based on the longer duration of trajectories of up to 5-10 days depending on the objectives of the studies), the other types of fields can be used too. For example, Mahura *et al.*, 2003a; Baklanov *et al.*, 2003 used the fast transport (i.e. they considered trajectories during the first day of transport) probability fields to evaluate potential receptor regions and its boundaries for the Kursk nuclear submarine lifting, transportation, and decommissioning operation during 2001-2002. Similarly, Mahura *et al.*, 1999; Saltbonis *et al.*, 2000; Mahura & Baklanov, 2003a used trajectories of short duration to estimate possibility of the rapid atmospheric transport and farthest reaching boundaries on a geographical map from the nuclear plants as well as other nuclear risk sites (submarine bases, spent nuclear fuel facilities, nuclear weapons test site) in the Euro-Arctic and North Pacific regions (Mahura & Baklanov, 2002; Mahura *et al.*, 2003c).

The use of the constructed probability fields (which, as we mentioned, can be based on trajectories of different duration) for the source points can allow: 1) to identify the most probable directions of atmospheric transport and spatial distribution of flow patterns from the source points; 2) to evaluate the farthest boundaries on a geographical map which might be reached during atmospheric transport; 3) to estimate and rank the levels, range, and probabilities of potential impact at the exact geographical receptor locations or specific receptor regions with defined borders.

3.6. PROBABILISTIC FIELDS ANALYSIS FOR RECEPTOR POINTS TO IDENTIFY SOURCE REGIONS

Similarly to the probabilistic fields for the source points such fields can be constructed for the receptor points in order to identify potential source regions. As shown in Fig. 3.6.1 for two Alaskan cities – Anchorage and Nome – we considered not only potential source regions but also included already known source points such as the Bilibino site (BNRS) and Kamchatka site (KNRS).

On an annual scale (3.6.1a), for Anchorage the potential remote source regions are located along the shore of the Arctic Ocean, in the North Pacific northerly of 35°N, and Russian Far East including the Chukotka region. Both the Bilibino and Kamchatka sites are within a 5-10% belt of the isolines of AHPPI, and hence, they represent a similar order of potential impact to Anchorage compared with Nome. On an annual scale (3.6.1b), for Nome the potential remote source regions are located in the central parts of the Arctic Ocean, in the North Pacific northerly of 40°N, and Russian Far East including the Chukotka region. The Bilibino site is within a 15-20% belt of the AHPPI isolines and represents the higher potential impact to Nome compared with the Kamchatka site, which is located only within a 5-10% belt.

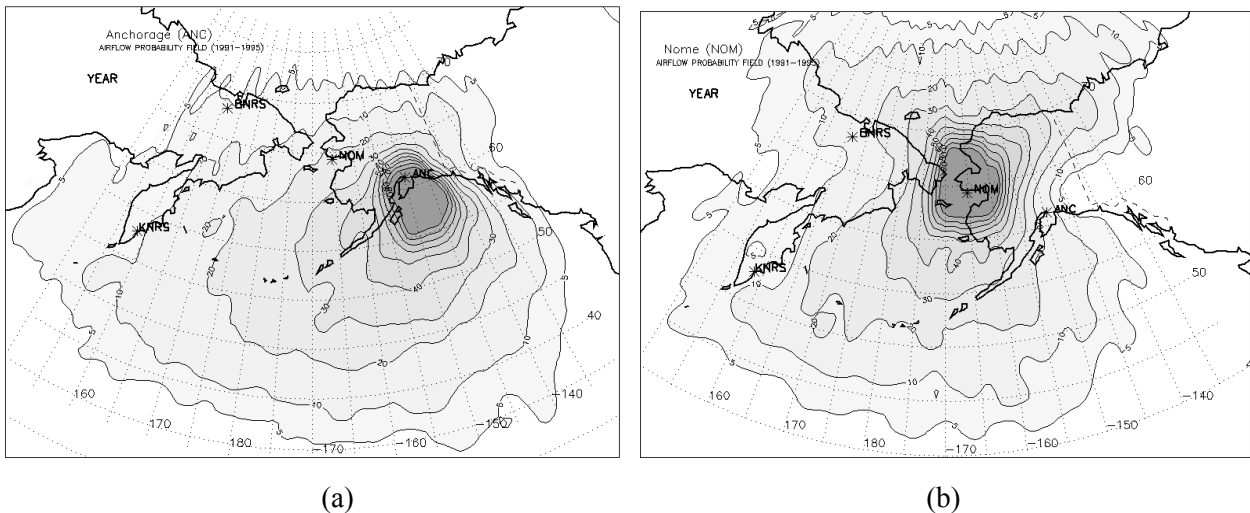


Figure 3.6.1. Annual air flow probability fields for the North Pacific sites (receptor points): a) Anchorage, State of Alaska, US and b) Nome, State of Alaska, US.

More detailed analysis of potential source regions can be done if air flow probability fields will be estimated when trajectories divided into groups by number of days of atmospheric transport. I.e. these fields can be constructed at individual time intervals when trajectories paths terminated at exact days. An example is shown in Fig. 3.6.2 for Anchorage. During the first day (0.5 and 1.0) there is the highest probability that a contaminated air mass will arrive from the S-SE sector of the city (from the Gulf of Alaska, from a distance of up to 1500 km). During next day (1.5 and 2.0 days before arrival at the city) the area of a region from where an air mass will arrive to city increased significantly, and especially in the western direction by almost 20 degrees, as well as in the southern direction by next 10 degrees. The extension toward the North America (i.e. to the east of the site) was the smallest compared with the later two. Further, the propagation of the source region in the southern and western directions continued with a significant extension of its boundaries and areas over the Gulf of Alaska and North Pacific Ocean aquatoria. Moreover, there is a separation into several source-subregions located mostly along the Aleutian Chain Islands.

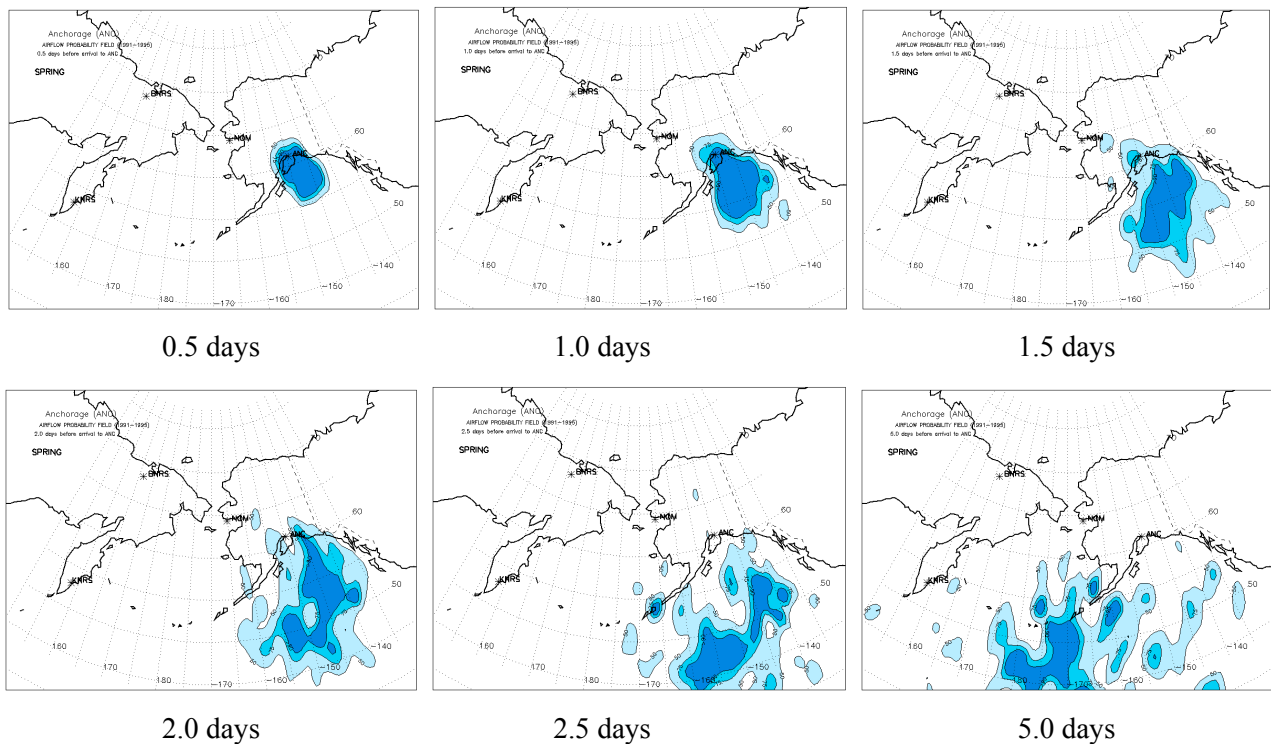


Figure 3.6.2. Spring airflow probability fields before arrival at Anchorage, Alaska at different time terms.

For the Mauna Loa observatory (MLO, located at 3.5 km asl; Hawaii, USA) there is a strong day-night breeze circulation, and hence, a contribution of different patterns of atmospheric regime might be underlined. Trajectories arrived during spring at the MLO site at different terms – 00 and 12 UTC - were analysed and they showed importance of the breeze circulation as well as presence of potential local sources on the observatory chemical measurement records.

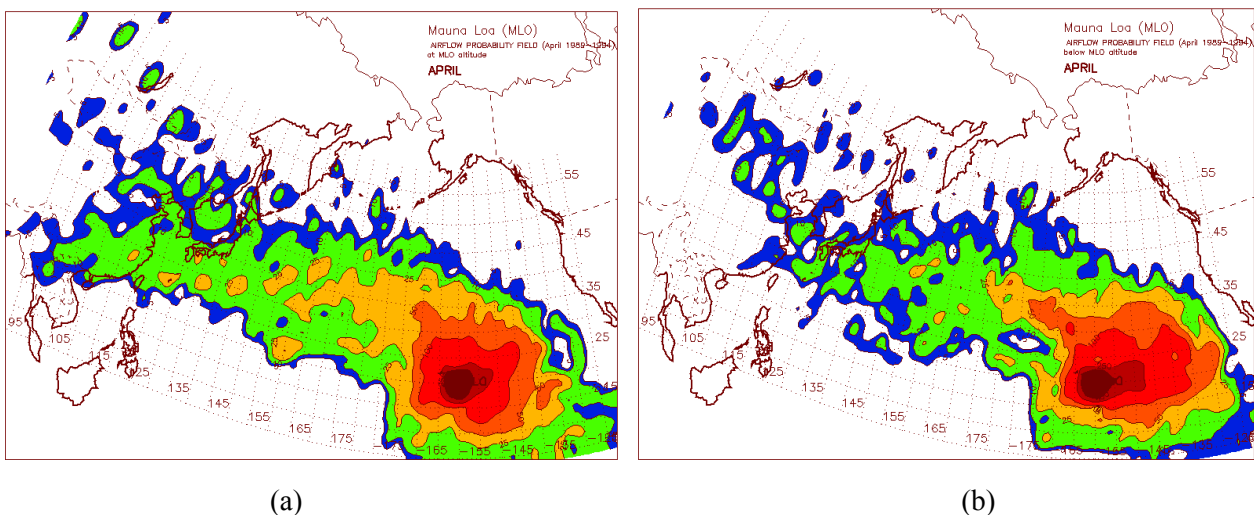


Figure 3.6.3. Airflow probability fields during April for the Mauna Loa observatory, Hawaii, US : a) at the site altitude of 3.5 km asl, and b) below the site altitude.

For investigation of importance of other sources rather than the well known Asian continent transport during spring, the analysis was done also at two levels: for trajectories arrived at altitude

of the MLO site (Fig. 3.6.3a) and for trajectories arrived below this altitude (Fig. 3.6.3b) during month of April, 1989-1994 (Mahura et al., 1997b). The examples of trajectories showing spring atmospheric transport from the Asian continent are shown in Fig. 3.6.3ab. The first figure shows atmospheric transport to the site with an origin within the boundary layer over the Indochina region of Asia, and the second figure shows trajectories with an origin within the free troposphere over the Asian continent. The Fig. 3.6.4c shows transport to MLO from the eastern direction – Central and North America - with an origin and a relatively slow transport within the boundary layer. Although during spring the later case is less often than the Asian continent transport, it still represents atmospheric transport from the industrialized countries, and hence, can not be neglected.

Moreover, if the lower altitudes of arrival at MLO site are considered (as shown in Fig. 3.6.3b) than there is significant change in the airflow patterns compared the higher altitude (as shown in Fig. 3.6.3a). First, the entire airflow field is more shifted from the Asian continent to the surrounding southern seas. Second, the clear presence of dominating transport from the eastern direction became evident although transport from the west also remained. This allows us to conclude that although during spring the Asian sources (such as dust transport, anthropogenic activity of rapidly developing Asian countries) are the major sources of pollution at MLO (as a receptor point), the other potential source regions such as the Central and North America should be also considered.

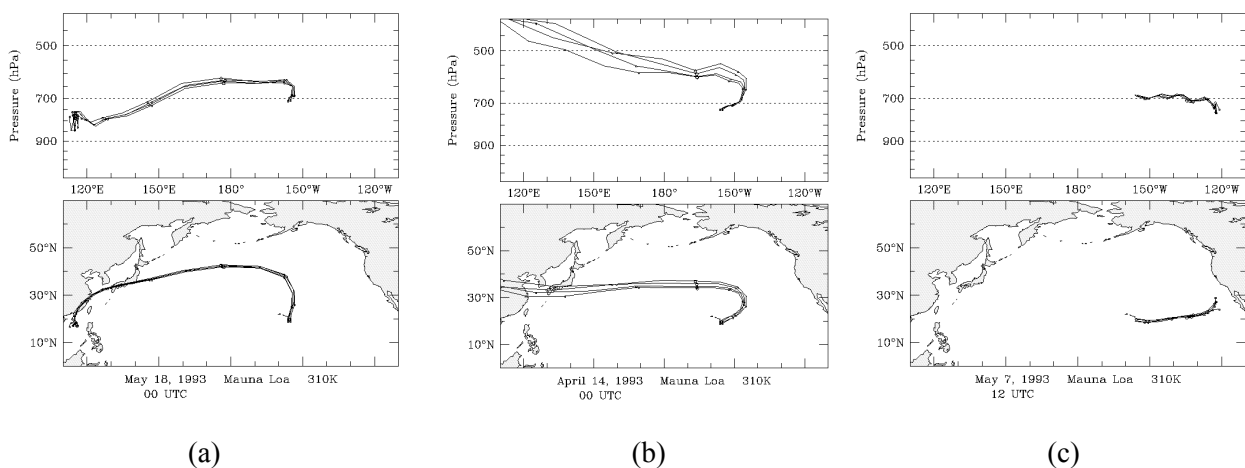


Figure 3.6.4. Isentropic trajectories showed atmospheric transport to the Mauna Loa observatory from the a) Asia, b) Asia, and c) Central and North America.

The use of such probability fields (which, as we mentioned, can be based on trajectories of different duration) for the receptor points can allow: 1) to identify the most probable directions of atmospheric transport to the receptor points/regions as well as spatial distribution of flow patterns arrived at receptor points; 2) to evaluate the farthest boundaries on a geographical map from where potential pollutants can arrive at the receptor site; 3) to estimate and rank the levels, range, and probabilities of potential impact from the source points/regions on a geographical map with respect to the receptor point.

3.7. COMBINED ANALYSIS OF PROBABILISTIC FIELDS FOR IDENTIFICATION OF SOURCE-RECEPTOR RELATIONSHIP

Let us consider individual airflow probability fields (e.g. during summer) for the source (Kamchatka) and receptor (Nome and Anchorage) points (shown in Fig. 3.7.1). The prevailing

flows for atmospheric transport from the Kamchatka site are westerlies which mainly transport air parcels through the Bering Sea and along the Aleutian Chain Islands. The dominating direction for air parcels arrivals at Nome is from the south-west of the site, i.e. from the aquatoria and surroundings of the Bering Sea. The dominating direction for air parcels arrivals at Anchorage is from the south of the site, i.e. aquatoria and surroundings of the Gulf of Alaska. For Nome there is a higher possibility of air parcels arrivals from the Arctic Ocean region compared with Anchorage.

The combinations of both summer airflow fields (source vs. receptor) are shown in Fig. 3.7.2. The intersections of airflow probability fields isolines showed a significant overlapping of these fields. As seen from Fig. 3.7.2a, during summer the possibility for an air parcel to leave the Kamchatka site region and arrive at Nome is high. Moreover, the rate of overlapping is the highest over the south-western parts of the Bering Sea, where it reaches a maximum of 50% of the area of the highest probability of possible impact (AHPPI) from the Kamchatka site as a source point, or 50% of the area of the remote potential impact (ARPI) for Nome as a receptor point. Let's call such interrelations (represented by overlapping between AHHPI and ARPI) as a sensitivity function field (represented by isolines of similar magnitudes and showing the areas and boundaries on a geographical map enclosed by these isolines). During summer the boundaries of the Nome airflow field are also more extended in the SE direction over the Gulf of Alaska.

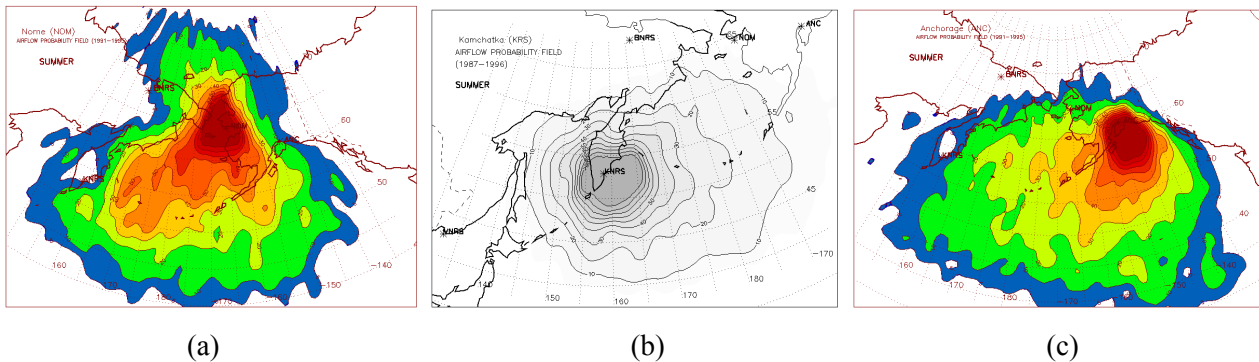


Figure 3.7.1. Summer airflow probability fields for a) Nome (receptor point), b) Kamchatka site (source point), and c) Anchorage (receptor point).

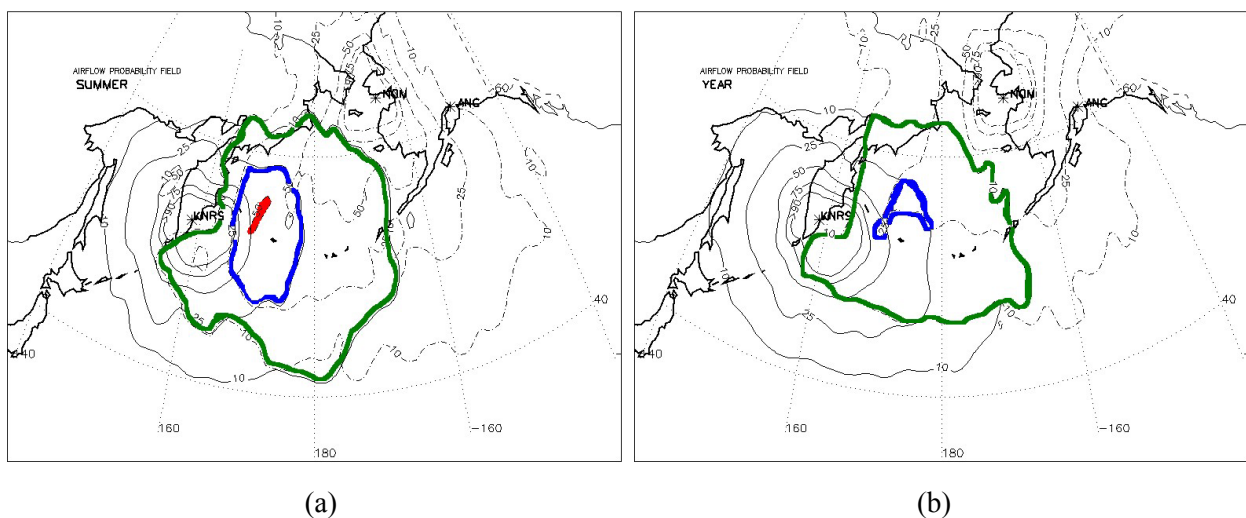


Figure 3.7.2. Overlapped airflow probability fields or sensitivity function for source vs. receptor points (Kamchatka site, Russia vs. Nome, Alaska) during: a) summer and b) year.

On an annual scale (3.7.2b), the higher ARPI values are mostly concentrated around Nome on a scale of a few hundred kilometres, although during summer it was extended to the south-west of the site on a scale of several thousand kilometres. The overlapping became less pronounced, and only isolines of 25% from both receptor and source sites crossed each other over the Bering Sea aquatoria between 170-180°E. The seasonal variability is an important factor and it showed that a difference in sensitivity might be doubled. Moreover, the annual area of this overlapping is almost 6 times smaller compared with summer. Throughout the year, the distance between the sites and the lowest isoline (10%) is higher (up to 6 times: ≈ 600 vs. 100 km) for Nome compared with the Kamchatka site. Hence, Nome, as a receptor point, will be more sensitive to releases at the Kamchatka site (as isoline of 10% passes along the shore of the Kamchatka Peninsula). Although for the source this Alaskan city will be considered to a lesser degree sensitive (as isoline of 10% passes farther south of the city over the Bering Sea).

As seen from Fig. 3.7.3a, during summer the possibility for an air parcel to leave the Kamchatka site region and arrive at Anchorage is not very high. Moreover, the rate of overlapping is the highest over the Bering Sea, where it reaches a maximum of 25% of the area of the highest probability of possible impact (AHPPI) from the Kamchatka as a source point, or 25% of the area of the remote potential impact (ARPI) for Anchorage as a receptor point. On an annual scale (3.7.3b), the higher ARPI values are mostly concentrated to the south of the city on a scale of up to 1000 km, similarly to the summer time. The overlapping became less pronounced, and only annual isolines of 10% from both sites crossed each other compared with summer season. Throughout the year, the distance between the points and lowest isoline (10%) is higher (up to 10 times: ≈ 1000 vs. 100 km) for Anchorage compared with the Kamchatka site. Similarly to Nome, Anchorage will be more sensitive to releases at the Kamchatka site (as isoline of 10% passes along the shore of the Kamchatka Peninsula). Although for the release site this city will be considered to a lesser degree sensitive (as isoline of 10% passes to the west of the site along the 175-170°W latitudinal belt).

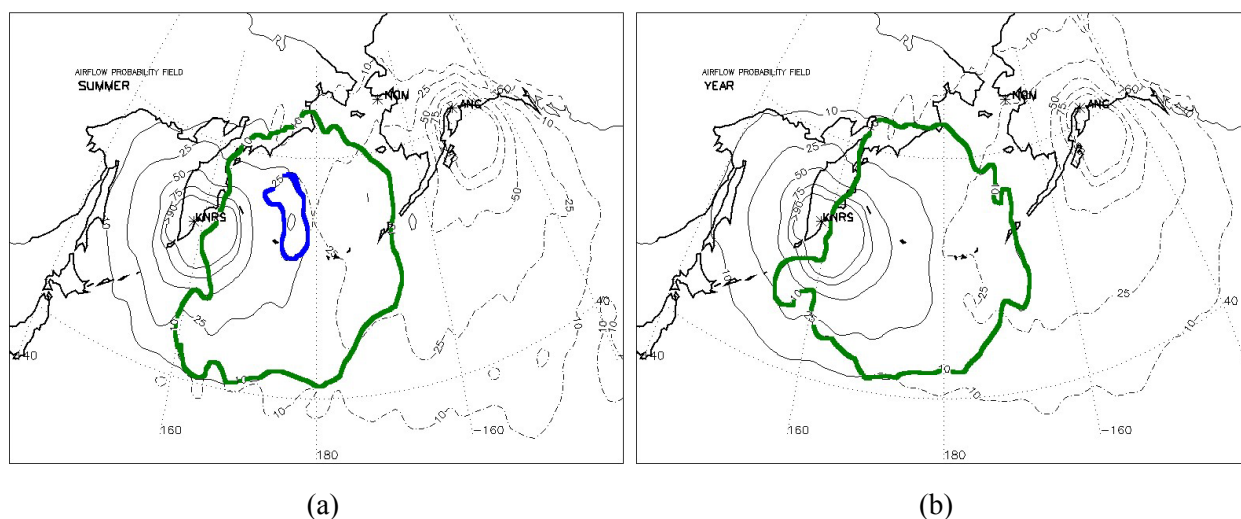


Figure 3.7.3. Overlapped airflow probability fields or sensitivity function for source vs. receptor points (Kamchatka site, Russia vs. Anchorage, Alaska) during: a) summer and b) year.

The use of combined fields for both receptor and source points simultaneously is more representative compared with a consideration of individual probability fields from/to source/receptor points discussed in §3.6 and 3.5. These averaging fields, called the sensitivity function fields can allow: 1) to identify the most probable directions and paths of atmospheric transport from/to source/receptor points/regions as well as spatial distribution of both flow patterns;

2) to underline the areas where the intersections of airflow fields occurred and where these intersections are more frequent; 3) to evaluate the farthest boundaries on a geographical map from where or to where potential pollutants can arrive; 4) if several sites are considered simultaneously when it is possible to estimate and rank the AHPPI and ARPI levels, range, and probabilities of impact from the source points/regions on a geographical map with respect to the receptor points; 5) to evaluate spatial distribution of sensitivity and its levels for source and receptor points with respect to each other.

It seems reasonable to mention that a more universal indicator, basing on a multiperiod calculated trajectories and representing simultaneously several important characteristics (described in §3.1-3.7) of the source-receptor relationship, is needed to be developed. This should include, at least, simultaneously information on a geographical map about each day of atmospheric transport and consist of the: 1) most probable boundaries of territories with the AHPPI and ARPI including calculation of enclosed areas, 2) probabilities and times of transport in each sector or along each atmospheric transport pathway from/to source/receptor points, 3) farthest geographical boundaries which might be reached, at least, by one trajectory, and others (Mahura *et al.*, 2004).

For probabilistic fields constructed based only on forward and backward trajectories (i.e. when only atmospheric transport is considered) and used in interpretation of source-receptor relationship there is a problem related to a question: *What occurs if during atmospheric transport the airborne pollutants will undergo the dry and wet deposition processes?* Does it change an identification of the source-receptor relationship for atmospheric pollutants?

This “if” question is a separate topic of research. Partially, for the source points of the Euro-Arctic region the temporal and spatial variability of individual fields of dry and wet deposition patterns of pollutants (considering radionuclides), which occurred during atmospheric transport, were considered by Mahura *et al.*, 2003d. More detailed study is planned within the frameworks of the INTAS Call-2003 proposal: “Source-Receptor Relationships for Atmospheric Pollutants Related to Environmental Risks in the NIS countries – Methodology and Applications” (INTAS-2003).

CONCLUSIONS AND RECOMMENDATIONS

The main aim of this pilot study was the analyses of different approaches to evaluate source-receptor relationship for atmospheric pollutants in the Euro-Arctic and North Pacific regions. The methodology included the simple trajectory modelling approach combined with statistical methods of cluster analysis and probability fields analysis. Among source points - the risk sites of potential danger and environmental impact, and among receptor points - the populated cities were selected.

The approaches for identification and interpretation of potential source and receptor regions were given considering only variability of the atmospheric transport patterns without consideration of possible losses of pollutants during transport. These analyses were presented from different prospective – from a simple point of view to more complex and detailed evaluation of relationship.

First, the individual forward/ backward trajectories originated/ arrived at selected source/ receptor points were used to evaluate the presence of potential receptor/ source regions and their approximate geographical boundaries. These trajectories represented atmospheric transport from/ to source/ receptor points for a particular date. The shortcoming of such approach is a limit to an underlined atmospheric transport at a particular date considered, which may not be representative when a long-term record of measurements or observations for analyses is available, and more common patterns in source-receptor relationship are under investigation. Therefore, it was reasonable to study: *What occurs when a longer period of measurement/ observation records is available and multiple trajectories are considered?*

Second, the clustered forward/ backward trajectories originated/ arrived at selected source/ receptor points were used to evaluate the existence of potential receptor/ source regions, their approximate geographical boundaries, average transport times to the regions, and probabilities of such transport. These clustered trajectories represent general atmospheric transport pathways from/ to the source/ receptor points averaged for a long-term multiperiod (month, season, annual, etc.). Moreover, the combined consideration of both types of clustered trajectories for both source and receptor points was investigated too, which provided more detailed information about the source-receptor relationship. The shortcoming of such approach is a limit to the underlined general directions of atmospheric transport pathways during a particular time period considered, which may not be representative because information about specificity of atmospheric flow between pathways is not available, and more detailed patterns in source-receptor relationship are under investigation. Therefore, it was reasonable to study: *What occurs **between** atmospheric transport pathways?*

Third, the individual probabilistic fields of atmospheric transport (such as airflow, fast transport, etc.) based on a multiperiod (month, season, annual, etc.) forward/ backward trajectories originated/ arrived at selected source/ receptor points were used to evaluate a spatial distribution of potential receptor/ source regions, their detailed geographical boundaries, dominating transport patterns, levels of potential impact, transport times, and probabilities. Moreover, the combined consideration of probabilistic fields for source and receptor points was investigated by introducing the sensitivity function of relationship between source and receptor points as well as estimation of its spatial distribution and levels of joint impact. The shortcoming of such approach is a limit to considering of only atmospheric flow patterns, which may not be “fully and completely” representative of the source-receptor relationship. Because, in addition to atmospheric transport and diffusion, the processes of deposition and removal by precipitation are not presented, although these can play a substantial role in re-evaluation of relationship. Therefore, it was reasonable proposing to study: *What occurs **if** during atmospheric transport the airborne pollutants will undergo the dry and wet deposition as well as chemical reactions processes?*

The suggested approaches and methods as well as obtained results can be used for emergency response, decision-making, scientific, educational, and informational purposes by the following organisations:

- National and international organisations, programmes, etc. performing monitoring and control of the pollution situation such as the IAEA, GAW, WMO RSMCs and International Data Centre of CTBTO/PrepCom; national Ministries of Health, of Agriculture, of Atomic Energy, of Natural Resources and Environmental Protection, of Civil Defence Affairs, Emergencies and Elimination of Consequences of Natural Disasters, etc.
- National and international emergency-response, administrative, decision-making, etc. services and organizations of local (city, object, site), regional (county, region, territory), governmental (country) levels where sources and receptors of pollution are situated;
- Research, educational, and public institutions and organisations for scientific, educational, informational, etc. purposes.

They can be used also for the following purposes:

- Applications in climate change, environmental pollution, dust events, volcano eruptions, natural hazards, etc.;
- Estimation of informative quality of monitoring systems and assessment of environmental quality, efficiency of environmental protection measures;
- Evaluation of sensitivity functions for selected areas and potential source risk sites for regional socio-economic planning and sustainable regional development;

- Estimation of potential risk and vulnerability of regions, consequences analysis, probabilistic assessment of local-, regional-, and long-range transport of pollution resulted from short-term accidental and continuous routine releases or discharges of pollution from NCB (nuclear, chemical, biological) and natural hazard sites;
- During evaluation and decision-making process for construction of a new facility or complex of enterprises posing potential risk of NCB contamination for neighbouring regions, environment, and population;
- Improvement in planning the emergency response and decision-making to potential accidental releases from risk site of nuclear, chemical, and biological danger.

ACKNOWLEDGMENTS

The authors are grateful to Drs. Leif Laursen and Jens Havskov Sørensen (Danish Meteorological Institute, Copenhagen), Olga Rigina (Danish Technological University), Ronny Bergman (Swedish Defence Research Authority, FOI, Umeå), Boris Segerståhl (Thule Institute, University of Oulu, Finland), John Merrill (University of Rhode Island, Graduate School of Oceanography, Narragansett, RI, USA), Joyce Harris (NOAA CMDL, CO, USA), Sergey Morozov and Michail Beloglazov (Kola Science Center, RAS, Apatity, Russia), Vladimir Penenko (Institute of Computational Mathematics and Mathematical Geophysics, Novosibirsk, Russia), Daniel Jaffe (University of Washington, Seattle, USA), Frank Parker and Keith Compton (International Institute for Applied Systems Analysis), Robert Andres (University of North Dakota, Space Studies Department, Grand Forks, ND, USA) for collaboration and constructive comments.

The computer facilities at the Danish Meteorological Institute (DMI), International Institute for Applied Systems Analysis (IIASA), and National Center for Atmospheric Research (NCAR, Boulder, CO, USA) have been used extensively in the study. The meteorological data archives from the NCAR facilities were used as input in the trajectory modelling.

Thanks to the computer consulting services at DMI, IIASA, and NCAR. The following software products had been used in this study: IDL, Matlab, SPSS, SAS, GMT, and NCAR Graphics.

Financial support of this study included the grants of the Nordic Arctic Research Programme (NARP) and the Nordisk Forskerutdanningsakademi (NorFA).

REFERENCES

- Anfossi, D., **1988**: Experimental study of transalpine transport of trace effluents: a comparison with synoptic trajectories of airflow. *Ist. di Cosmogeofis., CNR, Turin Il Nuovo Cimento*, Bologna, 11C(5/6): 489-526.
- Anfossi, D., Sacchetti, D., **1994**: Transport of volcano Etna emissions towards the alpine region using ECMWF data. *Geophysics and Space Physics*, Bologna, Italy, 17C(4): 473-484.
- AR-NARP, **2001-2003**: On-going Project Atmospheric Transport Pathways, Vulnerability and Possible Accidental Consequences from the Nuclear Risk Sites in the European Arctic (*Arctic Risk*) of the NARP: Nordic Arctic Research Programme. WWW-site: <http://www.dmi.dk/f+u/luft/eng/arctic-risk/main.html>.
- Artz, R.S., Dayan, U., **1986**: Analysis and assessment of precipitation chemistry at Caribou, Maine. *Technical Memorandum (NOAA TM ERL ARL-143)*, March 1986, 62 p.
- Austin, J., Butchart, N., **1989**: Study of air particle motions during a stratospheric warming and their influence on photochemistry. *Royal Meteorological Society, Bracknell, Eng., Quarterly Journal*, 115(488, Pt. A): 841-866.
- Baklanov, A. **2000**: Modelling of the atmospheric radionuclide transport: local to regional scale. *Numerical Mathematics and Mathematical Modelling*, INM RAS, Moscow, Vol. 2 (Special Issue dedicated to 75-year Jubilee of Academician G.I. Marchuk), pp. 244-266.
- Baklanov, A., J. H. Sørensen, **2001**: Parameterisation of radionuclide deposition in atmospheric long-range transport modelling. *Physics and Chemistry of the Earth:(B)*, Vol. 26, No. 10, pp. 787-799.
- Baklanov A., Mahura A., **2001**: Atmospheric Transport Pathways, Vulnerability and Possible Accidental Consequences from the Nuclear Risk Sites: Methodology for Probabilistic Atmospheric Studies. *Danish Meteorological Institute Scientific Report*, #01-9. ISBN: 87-7478-450-1, 43p.
- Baklanov A., Mahura A., Sørensen, J.H., Rigina, O., Bergman, R., **2002**: Methodology for Risk Analysis based on Atmospheric Dispersion Modelling from Nuclear Risk Sites. NARP Arctic Risk project. *Danish Meteorological Institute Scientific Report*, 02-16, ISBN:87-7478-470-6, 54p.
- Baklanov, A., A. Mahura, J.H. Sørensen, **2003**: Methodology for Prediction and Estimation of Consequences of Possible Atmospheric Releases of Hazardous Matter: 'Kursk' Submarine Study. *Atmospheric Chemistry and Physics*, 3, 1515-1556.
- Bowman, K.P., **1995**: Diffusive transport by breaking waves. *Journal of the Atmospheric Sciences*, 52(13): 2416-2427.
- Chipperfield, M. P., Lutman, E. R., Kettleborough, J. A., Pyle, J. A., Roche, A. E., **1997**: Model studies of chlorine deactivation and formation of ClONO₂ collar in the Arctic polar vortex. *Journal of Geophysical Research*, 102(D1): 1467-1478.
- Clarke, J.F., **1983**: Assessment of model simulation of long-distance transport. *Atmospheric Environment*, 17(12): 2449-2462.
- De Pena, R.G., **1986**: Application of trajectory analysis to the assessment of local and long-range contributions to acidic deposition. *Water, Air, and Soil Pollution*, Dordrecht, Holland, 30(3/4): 885-896, Oct., 1986. (*International Symposium on Acidic Precipitation, Muskoka, Ontario, Sept. 15-20, 1985, Proceedings*)
- Dorling, S.R., Davies, T.D., Pierce, C.E., **1992**: Cluster analysis: a technique for estimating the synoptic meteorological controls on air and precipitation chemistry results from Eskdalemuir, South Scotland. *Atmospheric Environment*. Part A: General Topics, 26A(14): 2583-2602.
- Elbern H., H. Schmidt, **1999**: A four-dimensional variational chemistry data assimilation scheme for Eulerian chemistry transport modelling. *J. Geophys. Res.*, 104, 18,583 - 18,598.

- Elbern H., H. Schmidt, **2002**: Chemical 4D variational data assimilation and its numerical implications for case study analyses. *IMA Volumes in Mathematics and its Applications*, Vol.130: Atmospheric Modeling, eds. David P. Chock, Gregory R. Carmichael, pp.165 - 184.
- Eluszkiewicz, J., **1996**: A three-dimensional view of the stratosphere-to-troposphere exchange in the GFDL SKYHI model. *Geophysical Research Letters*, 23(18): 2489-2492.
- Fosberg, M.A., **1984**: Transport and diffusion in the transition layer and planetary boundary layer for drainage flows in Anderson and Putah creeks, California, during ASCOT 1980. *Journal of Climate and Applied Meteorology*, 23(5): 812-823.
- Gorodnichi D.O., Reznik A. M. **1997**: Increasing Attraction of Pseudo-Inverse Autoassociative Networks. *Neural Processing Letters*, V.5, #2, pp.123-127.
- Haagenson P.L., Tschudy K.L., Skumanich M., Seaman N.L., **1987**: Tracer verification of trajectory models. *Journal Clim. Appl.*, Vol.26, pp.410-426.
- Haagenson, P.L., **1985**: Relationship between acid precipitation and three-dimensional transport associated with synoptic-scale cyclones. *Journal of Climate and Applied Meteorology*, 24(9): 967-976.
- Harris J.M., Kahl J.D. **1990**: A descriptive atmospheric transport climatology for Mauna Loa Observatory, using clustered trajectories. *Journal of Geophysical Research*, pp.13,651-13,667.
- Harris, J.M., Tans, P.P., Dlugokencky, E.J., Masarie, K.A., Lang, P.M., Whittlestone, S., Steele, L.P., **1992**: Variations in atmospheric methane at Mauna Loa Observatory related to long-range transport. *Journal of Geophysical Research*, 97(D5): 6003-6010.
- Harris J.M., **1992**: An analysis of 5-day midtropospheric flow patterns for the South Pole: 1985-1989. *Tellus*, 44(B), pp.409-421.
- Harris J.M. and Kahl J.D., **1994**: Analysis of 10-day isentropic flow patterns for Barrow, Alaska: 1985-1992. *Journal of Geophysical Research*, Vol.99, 25,845-25,855.
- Harris, J.M., Oltmans, S.J., **1997**: Variations in tropospheric ozone related to transport at American Samoa. *Journal of Geophysical Research*, 102(D7): 8781-8791.
- Hass H., M. Memmesheimer, H. Geiss, H. J. Jakobs, M. Laube, A. Ebel, **1990**: Simulation of the Chernobyl radioactive cloud over Europe using the EURAD model. *Atmospheric Environment*, 24A, 673 - 692.
- INTAS, **2003**: INTAS Call-2003 proposal: "Source-Receptor Relationships for Atmospheric Pollutants Related to Environmental Risks in the NIS countries – Methodology and Applications" (PI: Dr. Alexander Baklanov).
- Jaffe, D, Mahura, A., Andres, R, **1997a**: Atmospheric Transport Pathways to Alaska from Potential Radionuclide Sites in the Former Soviet Union. *Research Report*, UAF-ADEC Project 96-001, p 71.
- Jaffe, D.A., Mahura A., Kelley, J., Atkins J., Novelli P.C., Merrill J., **1997b**: Impact of Asian Emissions on the Remote North Pacific Atmosphere: Interpretation of CO Data from Shemya, Guam, Midway and Mauna Loa. *J.Geophys.Res.*, 23, 28,627-28,636.
- Jaffe, D.A., L.N. Yurganov, E. Pullman, J. Reuter, A. Mahura, P.C. Novelli., **1998**: Measurements of CO and O₃ at Shemya, Alaska. *J.Geophys.Res.*, 103, 1493-1502.
- Janish, P.R., Lyons, S.W., **1992**: NGM performance during cold-air outbreaks and periods of return flow over the Gulf of Mexico with emphasis on moisture-field evolution. *Journal of Applied Meteorology*, 31(8): 995-1017.
- Kahl J.D., Samson P.J., **1986**: Uncertainty in trajectory calculations due to low resolution meteorological data. *Atmospheric Environment*, 25, 1816-1831.
- Kahl J.D., Samson P.J., **1988**: Uncertainty in estimating boundary-layer transport during highly convective conditions. *Journal Clim. Appl. Meteorol.*, Vol.27, pp.1,024-1,035.
- Kahl, J.D., **1996**: On the prediction of trajectory model error. *Atmos. Environ.* 30, 2945-2957.

- Kahl, J.D. W., Martinez, D.A., Kuhns, H., Davidson, C.I., Jaffrezo, J-L., Harris, J.M. (1997): Air mass trajectories to Summit, Greenland: a 44-year climatology and some episodic events. *Journal of Geophysical Research*, 102(C12): 26861-26875.
- Katsoulis, B. D., Whelpdale, D. M., 1993: A climatological analysis of four-day back trajectories from Aliartos, Greece. *Theoretical and Applied Climatology*, New York, NY, 47(2): 93-103.
- Kovalets I.V., Maderich V.S., 2001a: Mathematical Modelling of Heavy Cold Gas Dispersion In The Atmospheric Boundary Layer. *Computational Technologies*, J. of the Institute of Computational Technologies of the RAS, the special issue Proc. of the Int. Conf. "Recent developments in Applied Mathematics and Mechanics. Theory, Experiment, Practice", V6, №2, pp.197-207, (in Russian).
- Kovalets I.V. Maderich V.S. 2001b: Numerical 3D Model of the Heavy Gas Dispersion in the Atmosphere With the Use of Conservative Splitting Schemes. *Applied Hydromechanics*, J. Of the Ukr. Institute of Hydromechanics UNAS, V3, pp.28-36 (in Russian).
- Kowol-Santen, J., 1998: Numerical analysis of transport and exchange processes in the tropopause region in mid latitudes. *Scientific Report*, Koln, Germany, Universitat zu Koln, 186 p.
- Mahura, A., Jaffe D., Andres, R., Dasher, D., Merrill, J. 1997a: Atmospheric Transport Pathways to Alaska from Potential Radionuclide Sites in the Former Soviet Union. Proceedings of American Nuclear Society *Sixth Topical Meeting on Emergency Preparedness and Response*, San Francisco, California, April 1997, Vol 1, p 173-174.
- Mahura A., Jaffe A., Zang Y., 1997b: Variability of Spring Atmospheric Transport Patterns at MLO, Hawaii. Short-Term Pilot Study, unpublished material, GI UAF.
- Mahura A., Jaffe D., 1998: Seasonal Variability of Atmospheric Transport Patterns during 1989-1994 for Elevated Concentrations of Pollutants at Guam. Short-Term Pilot Study, unpublished material, GI UAF.
- Mahura A., R.Andres, Jaffe D., 1998: Atmospheric Transport Patterns from the Kola Nuclear Reactors. *UAF-INE-UW-CERUM Joint Project*, Fall 1998, 32 p.
- Mahura A., D.Jaffe, R.Andres, 1999: Air Flow Patterns and Precipitation Probability Fields for the Kola NPP. Abstracts of the International Conference "Nuclear Risks, Environmental and Development Cooperation in the North of Europe", Apatity, Russia, 19-23 June 1999, pp. 87-93.
- Mahura A., 2001: Probabilistic Assessment of Atmospheric Transport Patterns from Nuclear Risk Sites, *Ph.D. Phys.&Math. Thesis*, Russian State Hydrometeorological University/ Kola Science Center, Russian Academy of Sciences, 172p. (in Russian)
- Mahura, A., Baklanov, A. 2002: Probabilistic Analysis of Atmospheric Transport Patterns from Nuclear Risk Sites in Euro-Arctic Region. *Danish Meteorological Institute Scientific Report*, 02-15, ISBN: 87-7478-469-2, 87p.
- Mahura A., A. Baklanov A., J.H. Sørensen, F.L. Parker, V. Novikov, K. Brown, K.L. Compton, 2002: Probabilistic Analysis of Atmospheric Transport and Deposition Patterns from Nuclear Risk Sites in Russian Far East. *International Institute for Applied Systems Analysis / Danish Meteorological Institute / Joint Scientific Report*, Fal 2002, 80p.
- Mahura A., Baklanov A., 2003a: Probabilistic Indicators of Atmospheric Transport for Emergency Preparedness. *Environment International*, (In Press).
- Mahura A., Baklanov A., 2003b: Evaluation Of Source-Receptor Relationship For Atmospheric Pollutants Using Probability Fields Analysis. EGU Assembly, France, Nice, April 2003.
- Mahura A., Baklanov A., Sørensen J. H., 2003a: Methodology for Evaluation of Possible Consequences of Accidental Atmospheric Releases of Hazardous Matter. *Radiation Protection Dosimetry*, Vol. 103, #2, pp. 131-139.
- Mahura A.G., Jaffe D.A., Harris J.M., 2003b: Identification of Sources for Atmospheric Pollutants in the Arctic Using Isentropic Trajectory Analysis. Submitted to *The Science of the Total Environment*, *Spr 2003 (In a peer-review process)*, 13.

- Mahura A.G., A.A. Baklanov, J.H. Sørensen, F.L. Parker, V. Novikov, K. Brown, K.L. Compton, **2003c**: Assessment of Atmospheric Transport and Deposition Patterns Related to Russian Pacific Fleet Operations. *Submitted to Environmental Monitoring and Assessment, Spr 2003 (In a peer-review process), 14p.*
- Mahura A., Baklanov A., Sørensen J.H., **2003d**: Long-Term Atmospheric Transport and Deposition Patterns from Nuclear Risk Sites in Euro-Arctic Region. *Danish Meteorological Institute, DMI Scientific Report, Fal 2003, 87p.*
- Mahura A., A. Baklanov A., J.H. Sørensen, F.L. Parker, K.L. Compton, **2004**: Combined Indicators of Risk Site Possible Impact during Atmospheric Transport. *Manuscript in Preparation, 14pp.*
- Marchuk G.I., **1982**: Mathematical Modelling in the Environmental Problems, Nauka, Moscow.
- Marchuk G.I., **1995**: Mathematical Modelling in the Environmental Problems, Nauka, Moscow. Adjoint Equations and Analysis of Complex Systems. Kluwer Academic Publishers, Dordrecht, 466 p.
- Market, P.S., Moore, J.T., **1998**: Mesoscale evolution of a continental occluded cyclone. *Monthly Weather Review*, 126(7): 1793-1811.
- Martin, D., Bergametti, G., Strauss, B., **1990**: On the use of the synoptic vertical velocity in trajectory model: validation by geochemical tracers. *Atmospheric Environment. Part A: General Topics*, 24A(8): 2059-2069.
- Martin, D., Mithieux, C. Strauss, B., **1987**: On the use of the synoptic vertical wind component in a transport trajectory model. *Atmospheric Environment*, 21(1): 45-52.
- Merrill J., Bleck R., Avila L., **1985**: Modeling atmospheric transport to the Marshall Islands. *Journal of Geophysical Research*, Vol. 90, pp. 12,927-12,936.
- Merrill J., Bleck R., Boudra D.B., **1986**: Techniques of Lagrangian Trajectory Analysis in Isentropic Coordinates. *Monthly Weather Review*, Vol 114, pp 571-581.
- Merrill J., **1994**: Isentropic airflow probability analysis. *Journal of Geophysical Research*, Vol.99, pp.25,881-25,889.
- Miller, J.M. **1981**: A Five-Year Climatology of Back Trajectories from the Mauna Loa Observatory, Hawaii. *Atmospheric Environment*, Vol 15, Iss 9, pp 1553-1558.
- Moody J.L., **1986**: The influence of meteorology on precipitation chemistry at selected sites in the Eastern United States. *Ph.D. thesis, Univ. Michigan, Ann Arbor*, 176 p.
- Moody J.L., Gallow J.N., **1988**: Quantifying the relationship between atmospheric transport and the chemical composition of precipitation on Bermuda. *Tellus*, 40(B), pp.463-479.
- Moody J.L., Oltmans S.J., Hiram Levy II, Merril J.T., **1995**: Transport Climatology of tropospheric ozone: Bermuda, 1988-1991. *Journal of Geophysical Research*, Vol.100, pp.7,179-7,194.
- Penenko V.V., E.A.Tsvetova, **2000**: Some aspects of solving interrelated problems of ecology and climate. *Journal Of Applies mechanics and Technical Physics*, Vol 41, N5, 2000, 907-914.
- Penenko V.V. **2001a**: Application of inverse modelling and sensitivity theory to air pollution studies. In: Air pollution modelling and its application XV (Borrego, Schayers, eds.), (2001); Kluwer Academic/Plenum Publishers, pp.329-336.
- Penenko V.V., **2001b**: Revaling regions of increased ecological vulnerability: concept and approached to its realization. *Atmos.Oceanoc Opt.* (2001), Vol 14, N 6-7, 545-548.
- Penenko, V., A. Baklanov, **2001**: Methods of sensitivity theory and inverse modeling for estimation of source term and environmental risk/vulnerability areas. *Lecture Notes in Computer Science (LNCS)*, Springer, V. 2074: 57-66.
- Penenko V.V., A. Baklanov, E. Tsvetova, **2002**: Methods of sensitivity theory and inverse modelling for estimation of source parameters. *Future Generation Computer Systems*, 18 (2002), 661-671.

- Penenko V.V., E.A. Tsvetova, **2002**: Methods and models for assessment of ecological risks. *Atmos. Oceanic Opt.* 2002, Vol 15, N5-6, 370-376.
- Perrin, G., Simmonds, I., **1995**: The origin and characteristics of cold air outbreaks over Melbourne. *Australian Meteorological Magazine*, 44(1): 41-59.
- Pudykiewicz, J. A., **1998**: Application of adjoint tracer transport equations for evaluating source parameters, *Atmos. Environ.* 32, pp. 3039-3050.
- Puhakka, T., **1988**: Meteorological factors influencing the radioactive deposition in Finland after the Chernobyl accident. In: *Finland. Dept. of Meteorology, Univ. of Helsinki, Report No. 29*, 49 p.
- Rizi, V., Redaelli, G., Visconti, G., Masci, F., Wedekind, C., Stein, B., Immler, F., Mielke, B., Rairoux, P., Woste, L., Del Guasta, M., Morandi, M., Castagnoli, F., Balestri, S., Stefanutti, L., Matthey, R., Mitev, V., Douard, M., Wolf, J. P., Kyro, E., Rummukainen, M., Kivi, R., **1999**: Trajectory studies of polar stratospheric cloud lidar observations at Sodankyla (Finland) during SESAME: comparison with box model results of particle evolution. *Journal of Atmospheric Chemistry*, 32(1): 165-181.
- Romesburg C.H., **1984**: Cluster Analysis for Researches. Lifetime Learning, Belmont, California, 334p.
- Rotunno, R., Skamarock, W.C., Snyder, C., **1994**: An analysis of frontogenesis in numerical simulations of baroclinic waves. *Journal of the Atmospheric Sciences*, 51(23): 3373-3398.
- Ruijgrok, W., Romer, F.G. **1993**: Aspects of wet, acidifying deposition in Arnhem: source regions, correlations and trends (1984-1991). *Atmospheric Environment. Part A: General Topics*, 27A(5): 637-653.
- Saltbones J., A.Foss, J.Bartnicki, **2000**: Threat to Norway from potential accidents at the Kola nuclear power plant. Climatological trajectory analysis and episode studies. *Atmospheric Environment*, Vol 34, Iss 3, pp. 407-41
- Schoeberl, M. R., Doiron, S.D., Lait, L.R., Newman, P.A., Krueger, A.J. **1993**: A simulation of the Cerro Hudson SO₂ cloud. *Journal of Geophysical Research*, 98(D2): 2949-2955.
- Seibert, P., **1999**: Inverse modelling of sulfur emissions in Europe based on trajectories. In: Kasibhatla, P., Heimann, M., Rayner, P., Mahowald, N., Prinn, R. G., Hartley, D. E. (eds.): Inverse methods in global biogeochemical cycles. *AGU Geophysical Monograph Series*, 114, pp. 147-154.
- Seibert, P., **2001**: Inverse modelling with a Lagrangian particle dispersion model: application to point releases over limited time intervals. In: Gryning, S. E., Schiermeier, F.A. (Eds.): *Air Pollution Modelling and its Application XIV*. Proc. of ITM, Boulder. New York: Plenum Press, 381-389.
- Slanina, J., A., Willem A. H., **1983**: Tracking the source regions for wet deposition in the Netherlands by a combination of cluster analysis and meteorological interpretation. In: *International Conference on Precipitation Scavenging, Dry Deposition, and Resuspension, 4th, Santa Monica, CA., Nov. 29-Dec. 3, 1983, Proceedings, Vol. 1, Precipitation scavenging, N.Y., Elsevier Science Publ. Co., Incorporated*, 1983, p. 239-246.
- Sparling, L. C., Kettleborough, J. A., Haynes, P. H., McIntyre, M. E., Rosenfield, J. E., Schoeberl, M. R., Newman, P. A., **1997**: Diabatic cross-ISENTROPIC dispersion in the lower stratosphere. *Journal of Geophysical Research*, 102(D22): 25817-25829.
- Stohl A., **1998**: Computation, accuracy and applications of trajectories - A review and bibliography. *Atmospheric Environment*, Vol 32, Iss 6, pp. 947-966
- Stohl A., S. Eckhardt, C. Forster, P. James, N. Spichtinger, P. Seibert, **2002**: A replacement for simple back trajectory calculations in the interpretation of atmospheric trace substance measurements. *Atmospheric Environment*, 36, 29, 4635-4648.
- Sørensen, J.H. **1998**: Sensitivity of the DERMA Long-Range Gaussian Dispersion Model to Meteorological Input and Diffusion Parameters. *Atmos. Environ*, Vol 32, pp. 4195-4206.
- Thompson, A. M., Pickering, K. E., McNamara, D. P., Schoeberl, M. R., Hudson, R. D., Kim, J. H., Browell, E. V., Kirchhoff, V. W. J. H., Nganga, D., **1996**: Where did tropospheric ozone over southern Africa

and the tropical Atlantic come from in October 1992? Insights from ROMS, GTE TRACE A, and SAFARI 1992. *Journal of Geophysical Research*, 101(D19): 24251-24278.

Uccellini, L.W., **1988**: Numerical model-based diagnostic study of the rapid development phase of the Presidents' Day cyclone. In: Seminar on the Nature and Prediction of Extra Tropical Weather Systems, ECMWF, Reading, Eng., Sept. 7-11, 1987, *Proceedings, Reading, Eng., European Centre for Medium-Range Weather Forecasts*, March, 1988, Vol. 1, p. 123-154.

Scientific Reports

Scientific reports from the Danish Meteorological Institute cover a variety of geophysical fields, i.e. meteorology (including climatology), oceanography, subjects on air and sea pollution, geomagnetism, solar-terrestrial physics, and physics of the middle and upper atmosphere.

Reports in the series within the last five years:

No. 99-1

Henrik Feddersen: Project on prediction of climate variations on seasonal to interannual timescales (PROVOST) EU contract ENV4-CT95-0109: DMI contribution to the final report: Statistical analysis and post-processing of uncoupled PROVOST simulations

No. 99-2

Wilhelm May: A time-slice experiment with the ECHAM4 A-GCM at high resolution: the experimental design and the assessment of climate change as compared to a greenhouse gas experiment with ECHAM4/OPYC at low resolution

No. 99-3

Niels Larsen et al.: European stratospheric monitoring stations in the Arctic II: CEC Environment and Climate Programme Contract ENV4-CT95-0136. DMI Contributions to the project

No. 99-4

Alexander Baklanov: Parameterisation of the deposition processes and radioactive decay: a review and some preliminary results with the DERMA model

No. 99-5

Mette Dahl Mortensen: Non-linear high resolution inversion of radio occultation data

No. 99-6

Stig Syndergaard: Retrieval analysis and methodologies in atmospheric limb sounding using the GNSS radio occultation technique

No. 99-7

Jun She, Jacob Woge Nielsen: Operational wave forecasts over the Baltic and North Sea

No. 99-8

Henrik Feddersen: Monthly temperature forecasts for Denmark - statistical or dynamical?

No. 99-9

P. Thejll, K. Lassen: Solar forcing of the Northern hemisphere air temperature: new data

No. 99-10

Torben Stockflet Jørgensen, Aksel Walløe Hansen: Comment on "Variation of cosmic ray flux and global coverage - a missing link in solar-climate relationships" by Henrik Svensmark and Eigil Friis-Christensen

No. 99-11

Mette Dahl Meincke: Inversion methods for atmospheric profiling with GPS occultations

No. 99-12

Hans-Henrik Benzoni; Laust Olsen; Per Høeg: Simulations of current density measurements with a Faraday Current Meter and a magnetometer

No. 00-01

Per Høeg; G. Leppelmeier: ACE - Atmosphere Climate Experiment

No. 00-02

Per Høeg: FACE-IT: Field-Aligned Current Experiment in the Ionosphere and Thermosphere

No. 00-03

Allan Gross: Surface ozone and tropospheric chemistry with applications to regional air quality modeling. PhD thesis

No. 00-04

Henrik Vedel: Conversion of WGS84 geometric heights to NWP model HIRLAM geopotential heights

No. 00-05

Jérôme Chenevez: Advection experiments with DMI-Hirlam-Tracer

No. 00-06

Niels Larsen: Polar stratospheric clouds micro-physical and optical models

No. 00-07

Alix Rasmussen: "Uncertainty of meteorological parameters from DMI-HIRLAM"

- No. 00-08
A.L. Morozova: Solar activity and Earth's weather. Effect of the forced atmospheric transparency changes on the troposphere temperature profile studied with atmospheric models
- No. 00-09
Niels Larsen, Bjørn M. Knudsen, Michael Gauss, Giovanni Pitari: Effects from high-speed civil traffic aircraft emissions on polar stratospheric clouds
- No. 00-10
Søren Andersen: Evaluation of SSM/I sea ice algorithms for use in the SAF on ocean and sea ice, July 2000
- No. 00-11
Claus Petersen, Niels Woetmann Nielsen: Diagnosis of visibility in DMI-HIRLAM
- No. 00-12
Erik Buch: A monograph on the physical oceanography of the Greenland waters
- No. 00-13
M. Steffensen: Stability indices as indicators of lightning and thunder
- No. 00-14
Bjarne Amstrup, Kristian S. Mogensen, Xiang-Yu Huang: Use of GPS observations in an optimum interpolation based data assimilation system
- No. 00-15
Mads Hvid Nielsen: Dynamisk beskrivelse og hydrografisk klassifikation af den jyske kyststrøm
- No. 00-16
Kristian S. Mogensen, Jess U. Jørgensen, Bjarne Amstrup, Xiaohua Yang and Xiang-Yu Huang: Towards an operational implementation of HIRLAM 3D-VAR at DMI
- No. 00-17
Sattler, Kai; Huang, Xiang-Yu: Structure function characteristics for 2 meter temperature and relative humidity in different horizontal resolutions
- No. 00-18
Niels Larsen, Ib Steen Mikkelsen, Bjørn M. Knudsen m.fl.: In-situ analysis of aerosols and gases in the polar stratosphere. A contribution to THESEO. Environment and climate research programme. Contract no. ENV4-CT97-0523. Final report
- No. 00-19
Amstrup, Bjarne: EUCOS observing system experiments with the DMI HIRLAM optimum interpolation analysis and forecasting system
- No. 01-01
V.O. Papitashvili, L.I. Gromova, V.A. Popov and O. Rasmussen: Northern polar cap magnetic activity index PCN: Effective area, universal time, seasonal, and solar cycle variations
- No. 01-02
M.E. Gorbunov: Radioholographic methods for processing radio occultation data in multipath regions
- No. 01-03
Niels Woetmann Nielsen; Claus Petersen: Calculation of wind gusts in DMI-HIRLAM
- No. 01-04
Vladimir Penenko; Alexander Baklanov: Methods of sensitivity theory and inverse modeling for estimation of source parameter and risk/vulnerability areas
- No. 01-05
Sergej Zilitinkevich; Alexander Baklanov; Jutta Rost; Ann-Sofi Smedman, Vasily Lykosov and Pierluigi Calanca: Diagnostic and prognostic equations for the depth of the stably stratified Ekman boundary layer
- No. 01-06
Bjarne Amstrup: Impact of ATOVS AMSU-A radiance data in the DMI-HIRLAM 3D-Var analysis and forecasting system
- No. 01-07
Sergej Zilitinkevich; Alexander Baklanov: Calculation of the height of stable boundary layers in operational models
- No. 01-08
Vibeke Huess: Sea level variations in the North Sea – from tide gauges, altimetry and modelling
- No. 01-09
Alexander Baklanov and Alexander Mahura: Atmospheric transport pathways, vulnerability and possible accidental consequences from nuclear risk sites: methodology for probabilistic atmospheric studies
- No. 02-01
Bent Hansen Sass and Claus Petersen: Short range atmospheric forecasts using a nudging procedure to combine analyses of cloud and precipitation with a numerical forecast model
- No. 02-02
Erik Buch: Present oceanographic conditions in Greenland waters

- No. 02-03
Bjørn M. Knudsen, Signe B. Andersen and Allan Gross: Contribution of the Danish Meteorological Institute to the final report of SAMMOA. CEC contract EVK2-1999-00315: Spring-to.-autumn measurements and modelling of ozone and active species
- No. 02-04
Nicolai Kliem: Numerical ocean and sea ice modelling: the area around Cape Farewell (Ph.D. thesis)
- No. 02-05
Niels Woetmann Nielsen: The structure and dynamics of the atmospheric boundary layer
- No. 02-06
Arne Skov Jensen, Hans-Henrik Benzon and Martin S. Lohmann: A new high resolution method for processing radio occultation data
- No. 02-07
Per Høeg and Gottfried Kirchengast: ACE+: Atmosphere and Climate Explorer
- No. 02-08
Rashpal Gill: SAR surface cover classification using distribution matching
- No. 02-09
Kai Sattler, Jun She, Bent Hansen Sass, Leif Laursen, Lars Landberg, Morten Nielsen og Henning S. Christensen: Enhanced description of the wind climate in Denmark for determination of wind resources: final report for 1363/00-0020: Supported by the Danish Energy Authority
- No. 02-10
Michael E. Gorbunov and Kent B. Lauritsen: Canonical transform methods for radio occultation data
- No. 02-11
Kent B. Lauritsen and Martin S. Lohmann: Unfolding of radio occultation multipath behavior using phase models
- No. 02-12
Rashpal Gill: SAR ice classification using fuzzy screening method
- No. 02-13
Kai Sattler: Precipitation hindcasts of historical flood events
- No. 02-14
Tina Christensen: Energetic electron precipitation studied by atmospheric x-rays
- No. 02-15
Alexander Mahura and Alexander Baklanov: Probabilistic analysis of atmospheric transport patterns from nuclear risk sites in Euro-Arctic Region
- No. 02-16
A. Baklanov, A. Mahura, J.H. Sørensen, O. Rigina, R. Bergman: Methodology for risk analysis based on atmospheric dispersion modelling from nuclear risk sites
- No. 02-17
A. Mahura, A. Baklanov, J.H. Sørensen, F. Parker, F. Novikov K. Brown, K. Compton: Probabilistic analysis of atmospheric transport and deposition patterns from nuclear risk sites in Russian far east
- No. 03-01
Hans-Henrik Benzon, Alan Steen Nielsen, Laust Olsen: An atmospheric wave optics propagator, theory and applications
- No. 03-02
A.S. Jensen, M.S. Lohmann, H.-H. Benzon and A.S. Nielsen: Geometrical optics phase matching of radio occultation signals
- No. 03-03
Bjarne Amstrup, Niels Woetmann Nielsen and Bent Hansen Sass: DMI-HIRLAM parallel tests with upstream and centered difference advection of the moisture variables for a summer and winter period in 2002
- No. 03-04
Alexander Mahura, Dan Jaffe and Joyce Harris: Identification of sources and long term trends for pollutants in the Arctic using isentropic trajectory analysis
- No. 03-05
Jakob Grove-Rasmussen: Atmospheric Water Vapour Detection using Satellite GPS Profiling
- No. 03-06
Bjarne Amstrup: Impact of NOAA16 and NOAA17 ATOVS AMSU-A radiance data in the DMI-HIRLAM 3D-VAR analysis and forecasting system - January and February 2003
- No. 03-07
Kai Sattler and Henrik Feddersen: An European Flood Forecasting System EFFS. Treatment of uncertainties in the prediction of heavy rainfall using different ensemble approaches with DMI-HIRLAM
- No. 03-08
Peter Thejll and Torben Schmith: Limitations on regression analysis due to serially correlated residuals: Application to climate reconstruction from proxies

No. 03-09

Peter Stauning, Hermann Lühr, Pascale Ultré-Guérard, John LaBrecque, Michael Purucker, Fritz Primdahl, John L. Jørgensen, Freddy Christiansen, Per Høeg, Kent B. Lauritsen: OIST-4 Proceedings. 4th Oersted International Science Team Conference. Copenhagen 23-27 September 2002

No. 03-10

Niels Woetmann Nielsen: A note on the sea surface momentum roughness length.

No. 03-11

Niels Woetmann Nielsen: Quasigeostrophic interpretation of extratropical cyclogenesis

No. 03-12

Alexander Baklanov: FUMAPEX – project kick-off meeting and first progress report. Integrated systems for forecasting urban meteorology, air pollution and population exposure, EVK4-CT-2002-00097

No. 03-13

Rasmus Tonboe, Søren Andersen, Leif Toudal: Anomalous winter sea ice backscatter and brightness temperatures

No. 03-14

Alexander Mahura, Alexander Baklanov, Jens Havskov Sørensen: Long-term probabilistic atmospheric transport and deposition patterns from nuclear risk sites in euro-arctic region. Arctic risk – project of the Nordic Arctic Research Programme (NARP)